

Numerical study of blow-up in solutions to generalized Korteweg-de Vries equations

C. Klein

Institut de Mathématiques de Bourgogne, Université de Bourgogne, 9 avenue Alain Savary, 21078 Dijon Cedex, France, Tel: 00333803 95858, Fax: 00333803 95869, christian.klein@u-bourgogne.fr

R. Peter

Institut de Mathématiques de Bourgogne, Université de Bourgogne, 9 avenue Alain Savary, 21078 Dijon Cedex, France

Abstract

We present a detailed numerical study of solutions to general Korteweg-de Vries equations with critical and supercritical nonlinearity. We study the stability of solitons and show that they are unstable against being radiated away and blow-up. In the L_2 critical case, the blow-up mechanism by Martel, Merle and Raphaël can be numerically identified. In the limit of small dispersion, it is shown that a dispersive shock always appears before an eventual blow-up. In the latter case, always the first soliton to appear will blow up. It is shown that the same type of blow-up as for the perturbations of the soliton can be observed which indicates that the theory by Martel, Merle and Raphaël is also applicable to initial data with a mass much larger than the soliton mass. We study the scaling of the blow-up time t^* in dependence of the small dispersion parameter ϵ and find an exponential dependence $t^*(\epsilon)$ and that there is a minimal blow-up time t_0^* greater than the critical time of the corresponding Hopf solution for $\epsilon \rightarrow 0$. To study the cases with blow-up in detail, we apply the first dynamic rescaling for generalized Korteweg-de Vries equations. This allows to identify the type of the singularity.

1 Introduction

1.1 Background and motivation

The celebrated Korteweg-de Vries (KdV) equation provides an asymptotic description of one-dimensional waves in shallow water in the long wave-length

limit. For shorter wavelengths the dispersion in the KdV equation is in general too strong compared to what is observed in applications. A possible approach to address this short-coming of the model equation KdV is to tilt the balance between nonlinearity and dispersion towards nonlinearity which leads to generalized KdV (gKdV) equations,

$$u_t + u^n u_x + \epsilon^2 u_{xxx} = 0; \quad (1)$$

here the parameter n in the nonlinearity is taken to be a positive integer, KdV corresponds to $n = 1$, the modified KdV (mKdV) equation to $n = 2$; the parameter ϵ is a small dispersion parameter. The gKdV equations have three conserved quantities, the L_1 and the L_2 norm of u (or the *mass* $M[u] = \|u\|_2^2$) and the energy,

$$E[u] = \int_{-\infty}^{\infty} \left(\frac{\epsilon^2}{2} u_x^2 - \frac{1}{(n+1)(n+2)} u^{n+2} \right) dx. \quad (2)$$

The KdV and mKdV equation are completely integrable which implies that they have an infinite number of conserved quantities. For general n , the gKdV equations have just the three conserved quantities mentioned above.

The introduction of a stronger nonlinearity in KdV equations increases its importance with respect to dispersion, but has the well-known effect that solutions to gKdV equations may have finite time blow-up for $n \geq 4$, i.e., a loss of regularity with respect to the initial data in the form of diverging norms of the solution. The global well-posedness of the Cauchy problem in H^1 was proven in [15,16]. The case $n = 4$ is critical in the sense that solutions to gKdV for $n < 4$ for sufficiently smooth initial data $u(x, 0) = u_0(x)$ are globally regular in time. The case $n = 4$ is also distinguished by the invariance of the mass under rescalings of the form $x \rightarrow x/\lambda$, $t \rightarrow t/\lambda^3$ and $u \rightarrow \lambda^{2/n}u$ with $\lambda = const$ which leave equation (1) invariant.

1.2 Basic mathematical properties of generalized Korteweg-de Vries equations

The gKdV equations have localized travelling wave solutions of the form $u = Q_c(x - x_0 - ct)$ with $x_0, c = const$ and with

$$Q_c(z) = \left(\frac{(n+1)(n+2)c}{2} \operatorname{sech}^2 \frac{\sqrt{cn}}{2\epsilon} z \right)^{1/n}. \quad (3)$$

Obviously we have $Q_c(z) = c^{1/n}Q(\sqrt{c}z)$, where we have put $Q = Q_1$. This simple scaling property of the *solitons* allows to concentrate on the case $c = 1$. If we refer in the following to the gKdV soliton, it is always implied that $c = 1$.

It was shown in [4] that these solitons are linearly unstable for $n \geq 4$. Note that the energy of the soliton vanishes for $n = 4$.

The initial value problem for gKdV for the L_2 critical case $n = 4$ has been studied in detail in a series of papers [30,31,34,32,33,39]. In these papers, it was shown that initial data u_0 with negative energy subject to the condition $u_0 \in H^1$, $\|Q\|_2 \leq \|u_0\|_2 < \|Q\|_2 + \alpha_0$ with $\alpha_0 \ll 1$ lead to a blow-up of the solution in finite or infinite time. For asymptotically decreasing data such that $\int_{x>1} x^6 u_0^2 dx < \infty$, it was proven that there is blow-up in finite time. In the cases with blow-up, the *universal blow-up profile* of the self-similar blow-up is given by the soliton Q (3). A variational argument [43] implies that H^1 initial data with subcritical mass $M[u_0] < M[Q]$ generate global in time solutions in H^1 .

The work on L_2 critical blow-up was recently continued in three articles by Martel, Merle and Raphaël [35,36,37] to which we refer the reader for details. The stability of the soliton was addressed in [35], where it was shown that the soliton is both unstable against blow-up and against being radiated away towards infinity. More precisely the authors gave (see Theorem 1.1 of [35]) the following

Theorem 1 (Martel, Merle, Raphaël (2013)) *Let \mathcal{T}_{α^*} be the set given by*

$$\mathcal{T}_{\alpha^*} = \left\{ u \in H^1 \text{ with } \inf_{\lambda_0 > 0, x_0 \in \mathbb{R}} \left\| u - \frac{1}{\lambda_0} Q \left(\frac{\cdot - x_0}{\lambda_0} \right) \right\|_2 < \alpha^* \right\}$$

and let \mathcal{A} be the set of initial data $u(x, 0) = u_0$ given by

$$\mathcal{A} = \left\{ u_0 = Q + \epsilon_0 \text{ with } \|\epsilon_0\|_{H^1} < \alpha_0 \ll 1 \text{ and } \int_{x>1} x^{10} \epsilon_0^2 dx < \infty \right\}, \quad (4)$$

where $0 < \alpha_0 \ll \alpha^* \ll 1$ are universal constants, and let $u_0 \in \mathcal{A}$. If $E[u_0] < 0$ and if $u(x, t)$ is not a soliton, then $u(x, t)$ blows up at the finite time t^* and $u(t) \in \mathcal{T}_{\alpha^*}$ for $t < t^*$. Then there exist a constant (with respect to t) $l_0(u_0) > 0$ and functions $L(t)$ and $x_m(t)$ such that for $t \rightarrow t^*$

$$u(x, t) - \frac{1}{\sqrt{L(t)}} Q \left(\frac{x - x_m(t)}{L(t)} \right) \rightarrow \tilde{u} \in L_2, \quad (5)$$

and

$$\|u_x\|_2 \sim \frac{\|Q'\|_2}{l_0(t^* - t)} \quad (6)$$

with Q from (3), where

$$L(t) \sim l_0(t^* - t), \quad x_m(t) \sim \frac{1}{l_0^2(t^* - t)}. \quad (7)$$

In addition it is shown in Theorem 1.2 of [35] that there are just three scenarios possible for initial data $u_0 \in \mathcal{A}$ (4): blow-up in finite time as detailed in theorem 1, the solution is identical to the soliton Q , or it leaves the set \mathcal{T}_{α^*} in finite time. In addition it is proven that the minimal mass for initial data to lead to a blow-up is the mass of the soliton. Note, however, that the theorem does not exclude the possibility that the solution u for initial data with smaller mass than the soliton leaves \mathcal{T}_{α^*} at some time $t_1 > 0$ and reenters it after some finite time $t_2 > t_1$, which means that it becomes almost solitonic again. In addition there is no statement in the theorem whether the blow-up profile (5) can be also observed for localized initial data with negative energy and a mass much larger than the soliton, i.e., for $u_0 \notin \mathcal{A}$. It is one of the motivations of this paper to address numerically these questions which have not yet been investigated analytically.

The picture is much less clear for the supercritical cases $n > 5$. It is just known that blow-up is possible in this case, but not for which initial data, and the precise mechanism of the blow-up is unknown. It was also shown in [4] that the soliton is unstable in this case, but the mechanism of the instability or of a blow-up is not rigorously established. Therefore numerical experiments have been carried out in [1,2,3] to address this issue. The basic idea of the numerical approach in these papers was to use cubic (or higher) splines for the spatial dependence and an implicit fourth order Runge-Kutta method for the time dependence (which we will also use for some code), essentially fourth order methods in time and space. The studied examples were periodic on $[0, 1]$, and the maximum of the initial data was localized at $x = 0.5$. To address the blow-up, an adaptive mesh refinement was used. The maximum of the solution was shifted manually every few time steps back to $x = 0.5$. When $\sqrt{h}\|u\|_{\infty}/\|u\|_2$ dropped below a prescribed tolerance, the mesh size h of the spatial grid was refined close to the maximum of the solution. The resolution in time was increased to keep some conserved quantity, essentially the numerically computed energy, at a prescribed accuracy, which was not easy to achieve. This technique allowed in [3] to trace the L_{∞} norm and certain L_p norms of the solution in cases with blow-up. It was possible with this numerical approach to study blow-up in the supercritical cases $n > 4$, but the identification of the asymptotic behavior for the critical case $n = 4$ was not conclusive. Similar experiments were carried out in the presence of dissipation in the equations. The adaptive mesh refinement was very effective in tracing blow-up, but the lack of resolution in the rest of the computational domain, due to a numerical approach of finite order and due to less powerful computers than accessible today, made it impossible to decide whether the observed small oscillations were numerical artifacts or true effects in the solution. This was for instance noted in [7] where the oscillations were seen as an artifact. In [7] the authors studied the gKdV equation for the case $n = 5$ with numerical (the same approach as in [3]) and asymptotic methods. This allowed to conclude that a self-similar solution acts as an attractor for blow-up as in the critical

case, but that this is not a rescaled soliton (3). Instead the blow-up profile is given by a solution vanishing for $|\xi| \rightarrow \infty$ of the ordinary differential equation (ODE)

$$-a_\infty \left(\frac{2}{n} U_\infty + \xi U_{\infty, \xi} \right) - v_\infty U_{\infty, \xi} + U_\infty^n U_{\infty, \xi} + \epsilon^2 U_{\infty, \xi \xi \xi} = 0, \quad (8)$$

where $U^\infty = U^\infty(\xi)$ is independent of t and where a_∞ and v_∞ are constants. The ODE (8) was studied in [7] and in more detail in [24]. Since it contains two free parameters, a best fit of the numerical gKdV solution to a numerically found asymptotically decreasing solution of (8) was performed in [7] confirming the validity of the approach. Note that this is in contrast to the L_2 critical case $n = 4$ for which theorem 1 was proven. There the blow-up profile is asymptotically given by the soliton Q_c (3) which only contains one free parameter c which can be fitted by the rescaling $Q_c(z) = c^{1/n} Q(\sqrt{c}z)$.

1.3 Small dispersion limit

The parameter ϵ in (1) appears in the study of the small dispersion limit $\epsilon \ll 1$ as in [9]. It can be seen as being introduced in the gKdV equation (1) with $\epsilon = 1$ by some initial data, which vary on large scales of order $1/\epsilon$. Studying the solution of gKdV for such initial data on large time scales of order $1/\epsilon$ can be achieved by a transformation $x \rightarrow x\epsilon$, $t \rightarrow t\epsilon$ which takes gKdV with $\epsilon = 1$ to the form (1). Note that this rescaling changes the mass of u by multiplication with a factor $1/\epsilon$, which will of course be taken into account when addressing conditions on the norm of the initial data in the context of blow-up studies formulated for $\epsilon = 1$.

It is known that solutions to the formal limit of (1) for $\epsilon = 0$, generalized Hopf equations, have for generic localized initial data a point of gradient catastrophe for some finite time t_c . At this point, also denoted as *hyperbolic blow-up*, the L_∞ norm of the solution stays finite in contrast to the L_∞ blow-up in solutions to gKdV for finite ϵ . An important feature of the small dispersion limit of nonlinear dispersive PDEs as gKdV is the appearance of a *dispersive shock*, a zone of rapid modulated oscillations in the vicinity of the point of gradient catastrophe of the solution to the dispersionless equation for the same initial data. This small dispersion limit was studied in [9] also numerically. It was found in [9] that for $t > t_c$ a dispersive shock is observed. But due to an instability in the time integration scheme (an *exponential time differencing method* (ETD)) in the numerical approach, which will be addressed in more detail elsewhere, it was not possible to decide whether there will be an L_∞ blow-up of the solution in finite time. It is one of the goals of the present paper to answer this question (which is equivalent to blow-up for initial data of large mass) and to show, that there is finite time blow-up at some time t^* which

is always greater than t_c . Moreover there will be always a dispersive shock in contrast to the corresponding situation of nonlinear Schrödinger equations, see [10]. With the numerical methods presented in this paper, it is possible to address both the dispersive shock and a blow-up with the necessary resolution. We show that for $n = 4$, the asymptotic description of theorem 1 still applies though the studied initial data are very far from the soliton.

In the small dispersion limit of generalized NLS equations, it was conjectured in [10] that the NLS solution for small ϵ is locally given near the critical time of the semiclassical solution by the *tritronquée* solution of the Painlevé I equation where x and t have to be rescaled by a factor $\epsilon^{4/5}$. It was found numerically in [10] that the same scaling in ϵ applies also for the blow-up time in the L_2 critical case. No dispersive shock is observed in this case. For gKdV equations it was conjectured in [9] that the gKdV solution near the break-up point of the generalized Hopf solution is given by a special solution to the so-called Painlevé I2 equation where t has to be rescaled by a factor $\epsilon^{4/7}$. An important question in the context of gKdV is whether a dispersive shock can be observed before an eventual blow-up and whether the Painlevé asymptotics near the critical time of the generalized Hopf solution plays a role up to blow-up.

As in [9] we discuss the initial data $u_0 = \beta \operatorname{sech}^2 x$ in the semiclassical limit $\epsilon \ll 1$. These data are motivated by the KdV soliton and have the advantage to be more rapidly decreasing than the gKdV soliton (3). Thus it is possible to analytically continue the solution (within numerical precision) as a periodic function on a smaller computational domain. This allows to use effectively higher resolutions in Fourier space. The critical time for solutions to the generalized Hopf equation (gKdV (1) for $\epsilon = 0$) for these initial data can be given in closed form:

$$t_c = \frac{(1 + 2n)^{n+1/2}}{(2n)^{n+1} \beta^n}. \quad (9)$$

Note that we use a different scaling of the gKdV equation here with respect to [9] (a factor 6 is missing in front of the nonlinearity), which leads to a different critical time. The energy (2) is obviously always negative for fixed β if ϵ is small enough.

1.4 Structure of the present work and main results

In this paper, we present a careful numerical study of soliton stability in the critical and supercritical cases, of the small dispersion limit $\epsilon \ll 1$, and of the asymptotic behavior in the cases with blow-up. To this end we employ a dual approach: a direct integration of the gKdV equation (1), and a dynamically rescaled gKdV equation (16) as detailed in the next section for cases

with blow-up. Since these numerical approaches are independent, they provide a mutual check of their respective accuracy. In all cases, we use a Fourier spectral method for the spatial dependence which is optimal for the smooth initial data we discuss here. For the direct integration of gKdV we apply an implicit fourth order Runge-Kutta method for the time dependence as in [3], for the dynamically rescaled gKdV equation (16) an ETD scheme of fourth order. This implies the use of two high order methods for space and time allowing for an efficient numerical solution of high accuracy. For the dynamical rescaling, we follow the approach presented in [38,29,28,40], as well as in the monograph [42], for numerical studies of the blow-up of solutions to the nonlinear Schrödinger equations (NLS). These numerical methods have proven instructive in the analytic description of blow-up in NLS systems. A similar approach was applied in [25,44,26], but there only the independent variables were rescaled. The rescaling allows a high resolution computation up to times very close to blow-up. Since the critical case $n = 4$ is expected to show the behavior (5) near blow-up, this implies that the blow-up is expected for $x_m \rightarrow \infty$. To address this problem, we solve the equation in a frame commoving with the maximum of the solution. In addition, the blow-up profile for $n = 4$ is reached algebraically in the rescaled time whereas an exponential dependence is expected for $n > 4$. Thus it is numerically extremely challenging to get close to the critical time t^* . But as will be shown in the paper, we get close enough to allow for some fitting to the theoretical predictions. To the best of our knowledge, we present here the first implementation of a fully dynamical rescaling for gKdV equations. In the case of very large mass of the initial data, the direct integration of the dynamically rescaled equation (16) suffers from numerical instabilities at the boundaries of the computational domains. As in [18,22,21,23] the quantities of the dynamical rescaling are obtained in these cases by postprocessing the data from the direct integration of the gKdV equation (1).

Our numerical simulations are compatible with the following conjectures about the analytic behaviour of the solution in the critical and supercritical case. For $n = 4$ we have

Conjecture 2 *Let Q be the soliton (3) and $u(x, t)$ be the solution of (1) for $n = 4$ for smooth initial data $u_0(x) \in L_2(\mathbb{R})$ of sufficiently large mass with a single maximum.*

- *If $E[u_0] > E[Q]$ and $\|u_0\|_2 < \|Q\|_2$, the solution is radiated away to infinity.*
- *If $E[u_0] < E[Q]$ and $\|u_0\|_2 > \|Q\|_2$, then there is a blow-up at the finite time t^* as detailed in theorem 1, even for initial data not in the class \mathcal{A} (4).*

This means that perturbations of the soliton with smaller mass than the soliton will be radiated away to infinity without coming close again to the soliton state (there is no refocusing of the mass). In the case of a blow-up, the theory by

Martel, Merle and Raphaël [35] gives the asymptotic description of the blow-up even for localized initial data with much larger mass than the soliton.

For the supercritical case $n > 4$, we confirm the numerical results by Bona et al. [3] and Dix and McKinney [7] for the appearance of blow-up, but can in addition reliably trace dispersive oscillations and dispersive shocks. We give via a dynamical rescaling an asymptotic description of the blow-up profile. The study can be summarized in the following

Conjecture 3 *Let P be the solution to the ODE (8) discussed in [24] and $u(x, t)$ be the solution of (1) for $n = 5$ for smooth initial data $u_0(x) \in L_2(\mathbb{R})$ of sufficiently large mass with a single maximum, then there is a blow-up at the finite coordinates (x^*, t^*) such that*

- $$u(x, t) - \frac{1}{L(t)^{2/n}} P\left(\frac{x - x_m(t)}{L(t)}\right) \rightarrow \tilde{u} \in L_2 \quad (10)$$

where the scaling factor L has for $t \sim t^*$ the form $L(t) = C(t^* - t)^{1/3}$ with $C = C(u_0)$ a constant depending on the initial data u_0

- the position x_m of the maximum has the asymptotic behavior

$$x_m(t) = \gamma L(t) + x^* \quad \text{as } t \nearrow t^* \quad (11)$$

where $\gamma = \gamma(u_0)$ is a constant depending on the initial data u_0 .

In the small dispersion limit $\epsilon \ll 1$, we show that there is always a dispersive shock in contrast to the NLS case, and that the scaling of the blow-up time follows an exponential law in ϵ . More precisely we find

Conjecture 4 *Let $u_0 \in L_2(\mathbb{R})$ be smooth initial data with a single maximum and $\epsilon \ll 1$. Then the solution to the gKdV equation (1) for $n \geq 4$ has a dispersive shock for t between $t \sim t_c$, the break-up time of the solution to the generalized Hopf equation, and the blow-up time t^* . The ϵ dependence of the blow-up time is given by*

$$t^*(\epsilon) = t_0^* \exp(\alpha\epsilon), \quad (12)$$

where $t_0^* > t_c$ and α are constant with respect to ϵ .

The paper is organized as follows: In section 2 we present the used numerical methods and perform tests. The L_2 critical case $n = 4$ is discussed in section 3. We study perturbations of the soliton, the small dispersion limit and blow-up. The same examples are studied in section 4 for the supercritical case $n = 5$. In both these sections we test the numerical approaches in the presence of blow-up and identify viable strategies to characterize the mechanism of the blow-up. This allows in section 5 to study initial data with larger mass for the example of the small dispersion limit with $\epsilon \ll 1$ and to determine the ϵ dependence of the blow-up time t^* .

2 Numerical methods

In this section we present the used numerical methods. Two approaches will be applied which complement each other: On one hand we directly integrate the gKdV equation for given initial data. With this code we study soliton stability and the small dispersion limit of gKdV. In the cases with blow-up, we use in addition for the first time a dynamical rescaling for the gKdV equation to study the blow-up in more detail and to identify the type of formed singularity. This approach can also be used a posteriori on the data obtained with the direct integration to identify scaling laws for certain norms near blow-up. The spatial dependence will be treated with a Fourier spectral method in all cases, the time integration with fourth order methods. Both codes will be tested at the example of the explicitly known soliton solutions (3). Since the approaches are independent, the consistency of results with both codes provides an additional test of the accuracy.

2.1 Direct numerical integration

The choice to use Fourier methods is based on the excellent approximation properties spectral methods have for smooth functions as the ones studied here. We will always consider initial data which are rapidly decreasing, and which can thus be analytically continued as periodic within the finite numerical precision if the computational domain is chosen large enough. Since we study here dispersive equations, it is also important that spectral methods minimize the introduction of numerical dissipation that might suppress dispersive effects. The *method of lines* approach implies that the partial differential equation (PDE) (1) will be approximated via a system of ODEs for the Fourier coefficients. The latter system is *stiff*² because of the third derivative in x , but has the advantage that the stiffness appears in the linear term of the equation,

$$\hat{u}_t = \mathcal{F}(u) + \mathcal{L}\hat{u}, \quad (13)$$

where $\mathcal{L} = \epsilon^2 ik^3$ and $\mathcal{F}(u) = -iku\widehat{u^{n+1}}/(n+1)$. For equations of the form (13), there are many efficient high-order time integrators, see e.g. [6,14,12,17,19], especially for diagonal \mathcal{L} as in the Fourier case. Thus the Fourier approach is not only very convenient for the spatial dependence, but allows also efficient time integration of high accuracy.

In [19], most of the studied integrators as in [14] are explicit and thus in general

² The term stiffness is used here to indicate that there are different timescales in the studied problem which make the use of explicit methods inefficient for stability reasons.

much more efficient than implicit integrators. It was shown, however, that an implicit Runge-Kutta of fourth order (IRK4), a two-stage Gauss scheme, could be competitive if the iteration is optimized. This method has also been used in [3,7]. Similar to [19] we apply a simplified Newton scheme to solve the nonlinear equations for the IRK4 scheme. In this form the iteration converges rapidly (at early times in 3 to 4 iterations) because the stiffness in this example appears in the linear part \mathcal{L} which is addressed explicitly. Note that in [3,7], too, a simplified Newton iteration was applied, which in this case was efficient, but approximate since the differentiation matrices were not diagonal. We apply this approach since it is robust up to an eventual blow-up of the solution whereas the explicit schemes used in [17] would require prohibitively small time steps to address stability issues to be discussed elsewhere. This is the reason why one could not get close enough to actual blow-up in [9] to uniquely identify it.

Accuracy of the numerical solution is controlled as discussed for instance in [17,19] via the numerically computed energy (2) which will depend on time due to unavoidable numerical errors. We use the quantity

$$\Delta = |E(t)/E(0) - 1| \tag{14}$$

as an indicator of the numerical accuracy (if $E(0) = 0$ we just consider the difference $|E(t) - E(0)|$). It was shown in [17,19] that the numerical accuracy of this quantity overestimates the L_∞ norm of the difference between numerical and exact solution by two to three orders of magnitude. A precondition for the usability of this quantity is sufficient resolution in Fourier space, i.e., a large enough number of Fourier modes.

We generally choose the number N of Fourier modes high enough such that they decrease to machine precision (10^{-16} here) for times much smaller than the time of blow-up. The number N thus depends on the size of the computational domain, $x \in [-\pi, \pi]D$ where the real constant D is chosen large enough to ensure ‘periodicity’ of the initial data in the sense discussed above. An occurrence of blow-up in the code is indicated by an increase of the Fourier modes for the high wave numbers which implies eventually a failure of the iterative solution of IRK4 relations to converge. We always choose the time step sufficiently small to ensure that the solution is obtained with machine precision for times much smaller than the blow-up time.

Remark 5 *The chosen time step in the case of a blow-up is always small enough that a lack of resolution in Fourier space constrains the accuracy. In other words, the presented resolution in time is always high enough that a further reduction of the time step does not change the presented result. The code also does not get decisively faster, if an adaptive scheme is used, since the iteration converges more rapidly for smaller time steps. Therefore instead of an adaptive scheme, with which we were experimenting, we reduce the size of*

the time step until the final recorded time (controlled via energy conservation) does not change anymore.

2.2 Dynamic rescaling

The results in [35] for the critical case $n = 4$ and the numerical studies [3,7] suggest that an L_∞ blow-up of solutions to gKdV is to be expected for initial data with negative energy and mass larger than the soliton mass. This can be numerically addressed by an adaptive approach, a rescaling of the coordinates and of the solution u by some time dependent factor L , which is supposed to vanish at the blow-up time. In addition it is convenient to address the fact that the maximum which eventually develops into the blow-up is moving in contrast to NLS cases where such techniques have been applied for self similar blow-up (for the description of the method and the results in the NLS case, we refer to [42] and references therein). Thus we also shift the x coordinate by $x_m(t)$, the location of the maximum, in order to keep it at a constant position in the transformed coordinates. In the case $n = 4$, the quantity x_m is expected to tend to infinity at blow-up. With the coordinate change

$$\xi = \frac{x - x_m}{L}, \quad \frac{d\tau}{dt} = \frac{1}{L^3}, \quad U = L^{2/n}u, \quad (15)$$

which leaves gKdV invariant for constant L and x_m , we get for (1)

$$U_\tau - a \left(\frac{2}{n}U + \xi U_\xi \right) - vU_\xi + U^n U_\xi + \epsilon^2 U_{\xi\xi\xi} = 0, \quad (16)$$

with

$$a = (\ln L)_\tau, \quad v = \frac{x_{m,\tau}}{L}, \quad (17)$$

where $x_{m,\tau}$ denotes the derivative of x_m with respect to τ . The coordinate transformation (15) implies in the cases studied here that a blow-up occurs at $\tau = \infty$. Thus the space and time scales are changed adaptively around blow-up, exactly in the way predicted by [35] for the critical case.

Equation (16) is also important for theoretical purposes and has been used in [30] and later works. In the limit $\tau \rightarrow \infty$, i.e., at blow-up, the functions U , v and a are expected to become independent of τ which is denoted by an index ∞ . For v this can be seen from the fact that $x_m \propto 1/L$ for $n = 4$ and that we find numerically that $x_m \sim \gamma L + x^*$ for $n = 5$ which implies that $v_\infty \propto a_\infty$ in both cases. Thus (16) is expected to reduce in the limit $\tau \rightarrow \infty$ to the ODE (8).

For the numerical implementation, the scaling factor L and the speed v have to be chosen in a convenient way. We choose ξ such that the maximum of $|U|$

is located at $\xi = \xi_0$ which implies $U_\xi(\xi_0, \tau) = 0$. This condition implies by differentiating (16) with respect to ξ ,

$$v = -a\xi_0 + U(\xi_0, \tau)^n + \frac{\epsilon^2 U_{\xi\xi\xi\xi}(\xi_0, \tau)}{U_{\xi\xi}(\xi_0, \tau)}. \quad (18)$$

The scaling function L on the other hand can be chosen to keep certain norms constant, for instance the L_∞ norm,

$$L^{2/n} = \frac{\|U\|_\infty}{\|u\|_\infty}. \quad (19)$$

We get from (16) in this case

$$a = \frac{n\epsilon^2 U_{\xi\xi\xi}(\xi_0, \tau)}{2 U(\xi_0, \tau)}. \quad (20)$$

Another possibility is to choose L such that the L_2 norm of U , which reads

$$L^{1/2-2/n} = \frac{\|U\|_2}{\|u\|_2}, \quad (21)$$

is constant. However, this is not convenient here since we also want to study the L_2 critical case $n = 4$ for which the L_2 norm is invariant under a rescaling of the form (15) (thus there is no condition on L in this case by imposing a constant L_2 norm of U). Alternatively one can impose that the L_2 norm of U_ξ is constant which is attractive since the blow-up theorems in [35] are formulated for this norm. In this case we have the relation

$$L^{2/n+1/2} = \frac{\|U_\xi\|_2}{\|u_x\|_2} \quad (22)$$

and we get by differentiating the norm with respect to t and by using equation (16) to eliminate derivatives with respect to t after some partial integrations

$$a = \frac{2n}{(n+1)(n+4)\|U_\xi\|_2^2} \int_{\mathbb{R}} U^{n+1} U_{\xi\xi\xi} d\xi. \quad (23)$$

For NLS computations with dynamic rescaling this approach proved to be numerically more stable than fixing the L_∞ norm to be constant, see [42] and references therein. We observe the same here. This appears to be due to the fact that condition (23) involves an integral over the whole computational domain, whereas condition (20) is local. In addition the appearance of the integral in (23) provides a global control of how well the numerical solution solves the rescaled equation (16). Therefore we will always apply the choice (23) in the following. Thus all quantities in (16) can be expressed in terms of U alone.

The spatial dependence in equation (16) will be again treated with Fourier spectral methods for the reasons outlined above. In addition the appearance of a fourth derivative in (16) implies that spectral accuracy is needed in the computation of the derivatives. Since the coordinate ξ is dynamically rescaled with respect to x , this implies that the computational domain has to be chosen large enough to avoid that the imposed periodicity of the solution affects the blow-up profile. As will be shown, this is possible for small enough masses except for the perturbed solitons where spurious oscillations in the quantity $a(\tau)$ appear which can be clearly attributed to the periodic boundary conditions. But due to the comparatively slow decrease of the soliton solution towards infinity, this case is problematic with any approach. Nevertheless we recover the predicted behavior of Theorem 1 [35] for $n = 4$. Note that the high spatial resolution also allows to avoid spurious oscillations as observed in [7] for the numerical study of blow-up in the supercritical case.

For the Fourier approach ξU_ξ in (16) is the numerically problematic term³. Since we have to choose large domains to address the ‘zooming in’ effect ($L \rightarrow 0$) at blow-up and since the solutions to (16) except for exact solitons have dispersive oscillations with slow decrease towards infinity, numerical errors at the boundaries for these *dispersive tails* lead to a pollution of the Fourier coefficients at the high frequencies. A damping of the oscillations at the boundaries is equivalent to imposing incorrect boundary conditions. These lead to reflections of the oscillations at the boundary which will eventually destroy the solution. A filtering in Fourier space to suppress an increase of the coefficients for high wave numbers has a similar effect. Thus the only way to address this problem without affecting the numerical solution appears to be the use of sufficient resolution in Fourier space and high time resolution, thus effectively propagating the solution with machine precision for as long as possible. As will be shown, this can be done for masses close to the soliton mass, but the needed resolution in time will become prohibitive once the mass is several times the soliton mass.

High time resolution can be achieved because equation (16) is in Fourier space again of the form (13). Since it is dynamically rescaled, there is no blow-up of the solution for finite τ . Thus we can use an explicit integrator. It was shown in [17] that ETD schemes perform best for KdV in the small dispersion limit, and in [19] that the performance is similar for different ETD schemes. The basic idea of these methods is to use a constant time step $h = t_{m+1} - t_m$ and to integrate (13) with an exponential factor,

$$\hat{u}(t_{m+1}) = e^{\mathcal{L}h} \hat{u}(t_m) + \int_0^h d\theta e^{\mathcal{L}(h-\theta)} \mathcal{F}(\hat{u}(\theta + t_m), \theta + t_m).$$

³ It is exactly this term which requires a special fall-off condition for the initial data in (4).

The different ETD schemes differ in the approximation of the integral. We use here the method by Cox and Matthews [6] which will be implemented as discussed in [17].

Note that the used ETD scheme is of classical order four (for a detailed discussion see [12,13]). But the information on the quantity a in (17) at the stages of the scheme is not of the same accuracy as at the full steps. Thus we only use a at the time steps t_n and obtain $\ln L$ via the trapezoidal rule which is of second order. Due to the high number of time steps we use in practice, L is obtained with more than sufficient accuracy. In the same way we obtain the time t from (15) and x_m from (18). To control the accuracy of both the numerical solution U and the computed factor L , we use that equation (16) has the conserved energy

$$E[U] = \frac{1}{L^{4/n+1}} \int_{-\infty}^{\infty} \left(\frac{\epsilon^2}{2} U_{\xi}^2 - \frac{1}{(n+1)(n+2)} U^{n+2} \right) d\xi. \quad (24)$$

Since $L(\tau)$ explicitly enters this quantity, $E[U]$ controls both U and L at the same time.

Remark 6 *It would be possible to use a transformation of the form $x \rightarrow x - x_m(t)$ also for the direct integration of gKdV to take care of the propagation of the maximum of the solution and to choose a commoving frame of reference. In this article we will always study positive initial data, i.e., the case which includes solitons. These propagate to the right. But except for the exact soliton solution, there will be dispersive oscillations also propagating to the left of the initial hump localized at 0. Thus resolution for a not commoving frame is needed in practice, or for one where the soliton is fixed close to the right boundary. A commoving frame is mainly beneficial in the context of a dynamical rescaling and will not be used for the direct integration of gKdV. In the latter case, we will sometimes place the initial hump closer to the right boundary at $\xi = \xi_0$ in order to leave maximal space to the dispersive oscillations propagating to the left.*

In cases of large mass where the solution of the rescaled equation (16) cannot be obtained close enough to the blow-up, we will directly integrate (1) as described in [18], and then postprocess the data to obtain the function L to identify blow-up. There are in principle two different cases important in this context, an algebraic or an exponential decay of the scaling factor L with τ . In the algebraic case observed for $n = 4$ we have $L(\tau) = C_1/\tau$ and thus $a_{\infty} = 0$. In this case the ODE (8) reduces to the ODE for travelling wave solutions of the gKdV equation in a commoving frame which has the unique localized solution Q (3) (recall that the soliton speed c can always be rescaled to 1). For $n > 4$ exponential decay $L(\tau) = C_2 e^{a_{\infty} \tau}$ with $C_2 = \text{const}$ is numerically observed which leads to $a_{\infty} < 0$ and thus to the ODE (8). Since we solve in this paper gKdV for small mass in the rescaled form (16) and since we observe

the expected behavior of the scaling factor $L(\tau)$, we solve for large τ also (8). For a given solution $u(x, t)$, the quantity $L(t)$ is determined either via (22) and the condition that $\|U_\xi(\cdot, 0)\|_2 = \|u_x(\cdot, 0)\|_2$ or via (15) and the condition that $\|U\|_\infty = \|u_0\|_\infty$. For an exponential dependence of L on τ , we have for $\tau \rightarrow \infty$

$$L \propto (t^* - t)^{1/3}, \quad \|u_x\|_2^2 \propto \frac{1}{(t^* - t)^{3/5}}, \quad \|u\|_\infty \propto \frac{1}{(t^* - t)^{2/15}} \quad (25)$$

and for an algebraic one

$$L \propto (t^* - t)^{1/2}, \quad \|u_x\|_2^2 \propto \frac{1}{t^* - t}, \quad \|u\|_\infty \propto \frac{1}{(t^* - t)^{1/4}}. \quad (26)$$

This allows to fit the L obtained from the norms of the solution to the expected asymptotic behavior. The L_2 norm of u_x involves an integral and thus takes into account the solution on the whole computational domain, whereas the L_∞ norm provides a local criterion. Consistency of the fitting results provides a test of the approach. In practice we run the codes until the conservation of the numerically computed energy drops below 10^{-3} which means the solution is no longer reliable. For the resulting data, we fit the last 1000 time steps to the expected asymptotic behavior (25) or (26). In the case of a linear dependence to be fitted, we use standard linear regression. For a nonlinear dependence as on t^* in (25) and (26), we apply the optimization algorithm [27] distributed with Matlab as *fminsearch*.

2.3 Tests of the numerics

Before using the above codes to study stability of the soliton solution (3) and the small dispersion limit of gKdV, we will first test with which accuracy the code can propagate the explicitly known soliton solution. It will be shown that this can be done essentially with machine precision which is important in view of the fact that the soliton is unstable against perturbations, which will be studied in the following sections. The fact that no instability is observed for the used methods on the studied timescales for the exact solution makes clear that a perturbation has to be considerably larger than the numerical error to lead to a visible effect for the considered times.

For the direct integration of gKdV for $\epsilon = 1$ with the IRK4 code, we use the initial data $Q(x+3)$ (3) and compute the solution until $t = 6$ for $x \in 10[-\pi, \pi]$. In this way we assure that the modulus of the Fourier coefficients for $N = 2^{10}$ Fourier modes decreases to 10^{-14} for $n = 4$ and 10^{-12} for $n = 5$ during the whole computation. If one wants to trace the solution for larger times with the same resolution, one has to use larger computational domains and a larger value of N . We use in both cases $N_t = 10^4$ time steps and find $\Delta \sim 6.46 * 10^{-15}$

for $n = 4$ as well as $\Delta \sim 1.07 * 10^{-13}$ (14) for the computation with $n = 5$. The difference between numerical and exact solution is $1.24 * 10^{-12}$ for $n = 4$ and $1.25 * 10^{-12}$ for $n = 5$. Note that the energy cannot be computed to higher precision than the resolution in Fourier space. This is why it is almost of the same order as the L_∞ norm of the difference between numerical and exact solution here.

We also test the code with dynamical rescaling for the soliton though in this case the function $L(t)$ will be equal to one within numerical precision. Nonetheless this test checks whether the code can propagate the soliton for finite times with machine precision in a commoving frame (due to the condition that the maximum is localized at $\xi = \xi_0$ with $\xi_0 = 0$, the soliton is stationary in this setting). The code is run up to $\tau = t = 100$ in this case, and the error is still of the order of 10^{-10} at the final time. There is no indication of an instability due to the numerical error on this timescale. The computation is carried out with $N = 2^{14}$ Fourier modes and $N_t = 2.5 * 10^5$ time steps for $x \in 100[-\pi, \pi]$. The computed energy is in this case of the order of 10^{-10} in accordance with the L_∞ norm of the difference between numerical and exact solution. The L_2 norm of U_ξ is constant to the order of 10^{-12} .

Since the numerical approaches for the direct integration of gKdV (1) and the dynamical rescaled equation (16) are independent, they can be used to test each other's quality. To illustrate this at a concrete example, we consider the case $n = 4$ for the initial data $u_0 = \text{sech}^2 x$ in the small dispersion limit $\epsilon = 0.1$, the example discussed in detail in section 3.2. There in Fig. 13, the solution obtained with the dynamically rescaled code is shown for $\tau = 1700$ which corresponds to $t = 4.1786 \dots$. We then use the code for the direct numerical integration of gKdV for the same initial data until exactly the same time (the parameters for the computation are given in section 3.2). In the latter case, the relative computed energy Δ is of the order of 10^{-7} , and the modulus of the Fourier coefficients decreases to 10^{-5} . Thus we estimate the solution to be accurate at least to the order of 10^{-4} . In the former case the relative computed energy is of the order of 10^{-4} , and the modulus of the Fourier coefficients decreases to the order of 10^{-8} . Thus we expect the solution to be accurate at least to the order of 10^{-3} . In fact if we plot both in dependence of x on the right in Fig. 1 by using the scaling (15), we see that both solutions cannot be really distinguished in the plot. Therefore we use cubic splines to interpolate from the grid in ξ to the one in x and present the difference of both solutions on the left in Fig. 1. It can be seen that this difference is smaller than 10^{-3} as expected. This provides as already mentioned a strong test of the numerical accuracy of both codes since we even have to interpolate between two grids. Thus we are convinced that all shown solutions in this paper are correct to at least plotting accuracy.

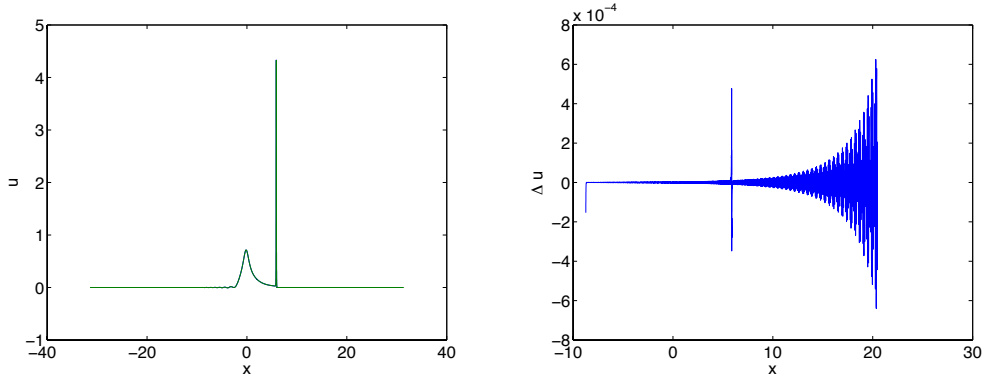


Fig. 1. Solution to the gKdV equation (1) for $n = 4$, $\epsilon = 0.1$ and the initial data $u_0(x) = \text{sech}^2 x$ for $t = 4.1786\dots$ in blue, and the solution to the rescaled gKdV equation (16) for $\tau = 1700$ after inverting the scaling (15) in green on the right; on the left we show the difference between both solutions.

3 The L_2 critical case $n = 4$ for small masses

In this section we study numerically solutions to the gKdV equation (1) in the L_2 critical case $n = 4$, where we concentrate on masses close to the soliton mass (up to three times the soliton mass). Cases with larger mass will be considered in section 5. We consider perturbations of the soliton and the limit of small dispersion. The results can be summarized as follows (see conjecture 2):

- Localized smooth initial data with a single maximum and a mass smaller than the soliton mass are radiated away to infinity (there is no refocusing of the solution).
- Initial data of this class with a mass larger than the soliton mass show self similar blow-up according to Theorem 1.

The limitation to masses of the same order as the soliton mass allows also to use two complementary numerical approaches which provides a strong test for the numerical methods, a direct integration of gKdV and the dynamical rescaling. In addition this study indicates how to address the case of larger masses in which the dynamical rescaled code is subject to numerical instabilities.

3.1 Perturbations of the soliton

We consider as initial data perturbations of the soliton (3) of the form $u(x, 0) = \sigma Q(x - x_0)$ with σ a real constant slightly smaller or bigger than 1, and x_0 the initial position of the soliton. This means that the initial data are in the class \mathcal{A} (4). In this subsection, we put $\epsilon = 1$. The mass of the soliton is $M[Q] = 6.0837\dots$ and its energy vanishes, $E[Q] = 0$.

We first consider the initial data $u(x, 0) = \sigma Q(x + 3)$, with $\sigma = 0.99$, on a large domain, $x \in 100[-\pi, \pi]$ with $N = 2^{14}$ Fourier modes and $N_t = 10^4$ time steps. In this situation the mass is obviously smaller than the mass of the soliton and the energy is positive. It can be seen in Fig. 2 that dispersive oscillations propagating to the left form immediately. The amplitude of these oscillations decreases very slowly which is why we choose a large computational domain. Only part of it is shown in the figure. It can be seen in Fig. 2 that the L_∞ norm of the solution for the perturbed soliton decreases in this case monotonically. Thus it appears that the soliton will be just radiated away, there is no indication of a refocusing of the mass which would not be excluded by theorem 1. The Fourier coefficients at the final time show that the solution is fully resolved in Fourier space. The energy is conserved in the computation to the order of 10^{-12} .

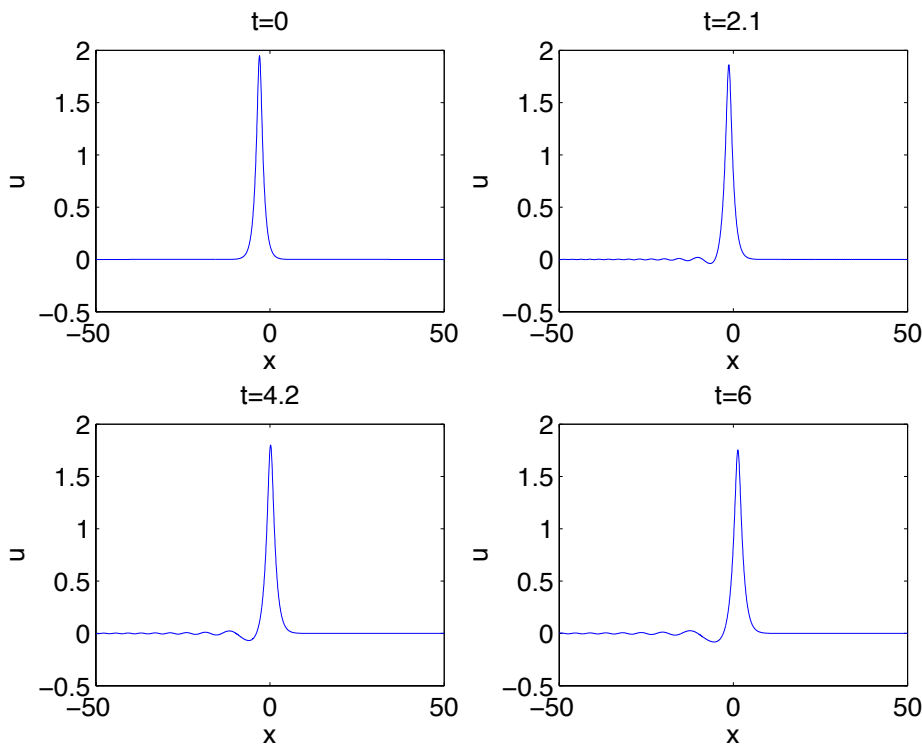


Fig. 2. Solution to the gKdV equation (1) with $\epsilon = 1$ for $n = 4$ and the perturbed soliton initial data $0.99Q(x + 3)$ (3) for several values of t .

The situation is completely different for initial data of the form $\sigma Q(x + 3)$ with σ slightly larger than 1. For $\sigma = 1.01$ we use $N_t = 2 * 10^5$ time steps for $t < 25$ whereas all other parameters are as above. Now the mass is larger than the soliton mass and the energy is negative. The code breaks at $t \approx 22.1814$ since the iteration no longer converges. But already at $t = 22.15$ the energy conservation used to check numerical accuracy drops below 10^{-3} . Thus we suppress the solution for larger times due to a lack of reliability. Note that

this is not our definition of the blow-up time, which will be determined below, it just delimits the set of reliable data generated with this set of parameters. The solution is shown for several times in Fig. 3. It can be seen that there will be again some dispersive oscillations propagating to the left. But more importantly the soliton becomes more and more peaked and thus travels at a higher and higher speed. At the same time it gets laterally compressed. Thus the solution behaves as predicted in [35] as a dynamically rescaled soliton.

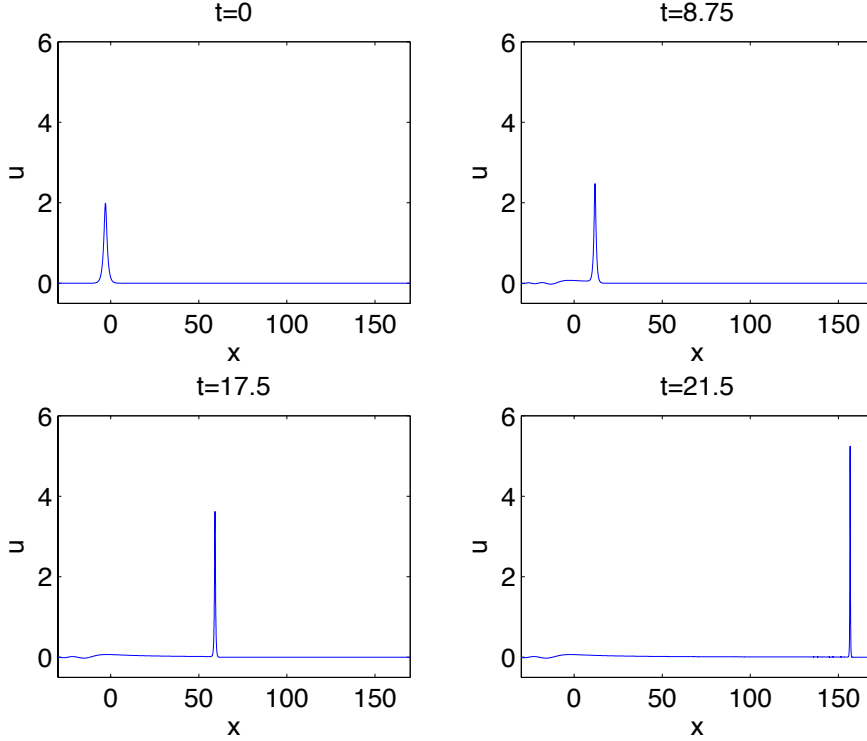


Fig. 3. Solution to the gKdV equation (1) with $\epsilon = 1$ for $n = 4$ and the perturbed soliton initial data $1.01 Q(x + 3)$ (3) for several values of t .

The increase of the L_∞ norm in Fig. 3 is even more obvious in Fig. 4. However the code with the used resolution is not able to get arbitrarily close to the blow-up time. As the Fourier coefficients at the final time in Fig. 4 show, this is not due to a lack of resolution in time but in space.

The slow increase of the L_∞ norm of the solution implies that it will not be possible to get much closer to the blow-up even with considerably higher resolutions in both time and space. But we can numerically check whether the analytical prediction that the L_∞ norm of the solution behaves close to blow-up as $\|u\|_\infty \sim (t^* - t)^\alpha$ with negative constant α . By fitting $\ln\|u\|_\infty$ to $\alpha \ln(t^* - t) + \kappa$, we find $\alpha = -0.4923$, $\kappa = 2.2803$ and $t^* = 25.0302$. The value of α is compatible with the theoretically predicted $-1/2$ (26). The difference between $\ln\|u\|_\infty$ and $\alpha \ln(t^* - t) + \kappa$ is below 1% and largest at the early

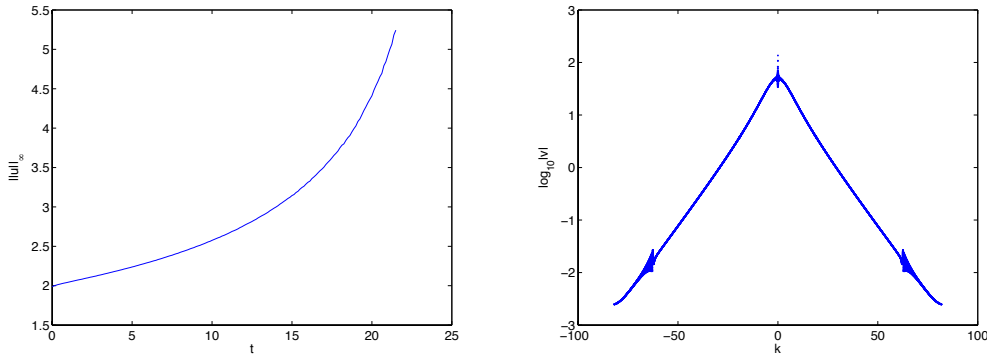


Fig. 4. L_∞ norm of the solution to the gKdV equation (1) with $\epsilon = 1$ for $n = 4$ and the perturbed soliton initial data $1.01 Q(x + 3)$ (3) in dependence of time on the left, and the modulus of the Fourier coefficients of the solution for $t = 21.5$ on the right.

times, but the values of the fitting parameters do not change much if the fitting is done only for larger times. This shows that the algebraic increase in time of the L_∞ norm of the solution is followed already for $t \ll t^*$ in good approximation. The fitting indicates a blow-up roughly for $t = 25$, whereas the code was stopped at $t = 22.15$.

The above results indicate as expected that the solution near blow-up is close to a rescaled soliton. Thus we solve the dynamically rescaled equation (16) for the same $\sigma = 1.01$ for $\tau \leq 500$ with $N_t = 2 * 10^6$ time steps and $N = 2^{16}$ Fourier modes for $\xi \in 1000[-\pi, \pi]$. The solution can be seen in Fig. 5. Since the maximum is fixed at $\xi = 0$, the dispersive oscillations propagate more rapidly to the left than is the case in Fig. 3. The plot suggests that the solution will be the rescaled soliton for $\tau \rightarrow \infty$, and that the remainder of the initial data will be radiated to infinity. The Fourier coefficients of the solution at the final time are also shown in Fig. 5 indicating that there is sufficient resolution in Fourier space. The relative computed mass is conserved to better than 10^{-4} . However, the energy conservation is only of the order of 10^{-2} . The comparatively low value of the latter is due to the dispersive oscillations reentering the computational domain and leading to a slight Gibbs phenomenon. Since the mass in contrast to the energy does not contain a derivative, it is less sensitive to this effect. Note that a slight increase of the computational domain does not change this decisively since the factor a tends only slowly to zero, and thus a reentering of the dispersive radiation cannot be suppressed in practice. In addition a larger domain increases the mentioned problems due to the term ξU_ξ in (16) which eventually lead to numerical instabilities even for prohibitively small time steps if the domain is too large.

The reentering of the computational domain of the dispersive oscillations due to the imposed periodicity has also an effect for the quantity $a(\tau)$ in Fig. 6. The slow increase of $a(\tau)$ to zero is superposed by oscillations due to the

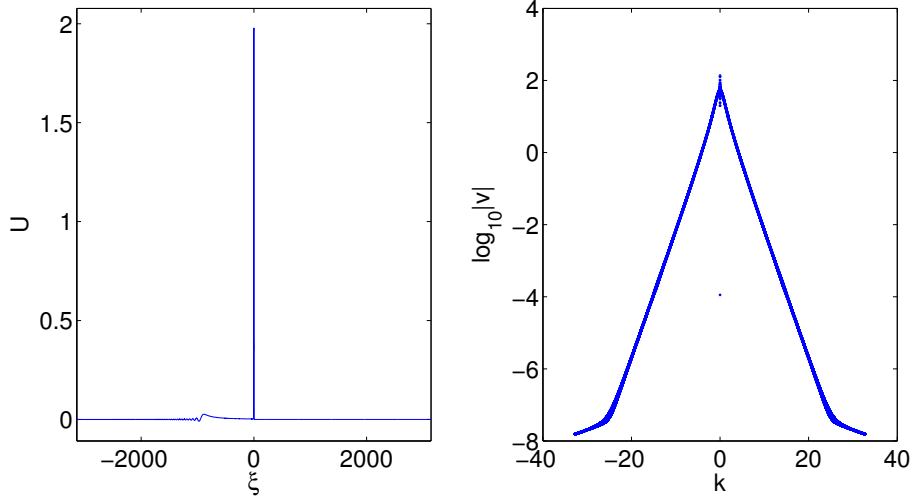


Fig. 5. The solution $U(\xi, \tau)$ of the equation (16) for the initial data $U(\xi, 0) = 1.01 Q(\xi)$ (3) for $\tau = 500$ (physical time: $t = 21.0787$) on the left and the corresponding Fourier coefficients on the right.

radiation emanating from the perturbed soliton. We only observe such spurious oscillations for perturbed soliton initial data since the latter and the generated dispersive oscillations decrease much slower than the $\text{sech}^2 x$ initial data. This is also the reason why we use a large domain and higher resolution in Fourier space to treat this case. Integrating $a(\tau)$ we obtain $L(\tau)$ and $t(\tau)$. Note that the spurious oscillations in $a(\tau)$ appear in both $L(\tau)$ and $t(\tau)$, but not if L is shown as a function of t . For larger values of t , the scaling factor L is as expected linear in t . Fitting as shown in Fig. 7 $L(t) = mt + L_0$ led to the values $m = -0.03931$ and $L_0 = 0.9861$ and thus to the blow-up time $t^* = 25.0836$, in accordance with the result from the fitting of the L_∞ norm of u from the direct solution of gKdV above. The L_∞ norm of the difference between L and its fit is of the order 10^{-4} .

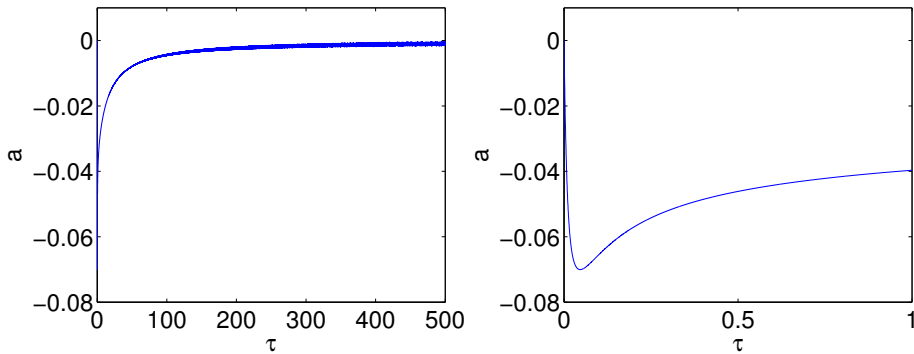


Fig. 6. The function $a(\tau)$ on the whole computed τ -range (left) and a close-up of $a(\tau)$ in the interval $\tau \in [0, 1]$ (right) for the solution of Fig. 5.

In Fig. 7 we also present the physical time t in dependence of the rescaled time τ . The plot shows that we do not get arbitrarily close to the blow-up time in

this example due to the fact that $a(\tau)$ tends slowly to 0, but close enough to extrapolate to the blow-up. This phenomenon was also observed in the case of the critical NLS equation [38,40,42].

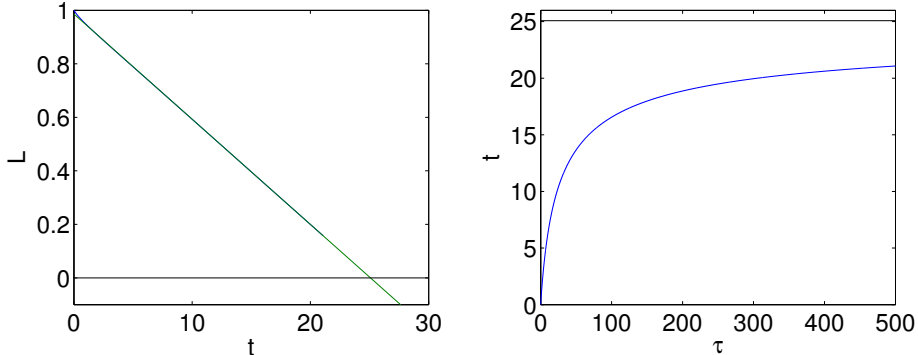


Fig. 7. The scaling factor L as a function of the physical time t and its fit for $t > 2$ to a straight line (left). The right figure shows the physical time as a function of the rescaled time τ . The black horizontal line in the right figure is the blow up time t^* determined from the fitting of L . Both figures correspond to the situation shown in Fig. 5.

The position of the maximum $x_m(\tau)$ and thus ultimately the location of the blow-up is shown in Fig. 8. As theoretically predicted, it tends to infinity. In the same figure we also present x_m in dependence of the physical time. A fit for small $t^* - t$ ($\ln(t^* - t) < 2.4$) for $\ln x_m \sim \gamma_2 \ln(t^* - t) + \ln(C_2)$ gives $\gamma_2 = -1.3282$ and $C_2 = 905.8$. It can be seen that the fitting for x_m is not as good as for the scaling factor L which is not surprising since the distance between the location of the blow-up and the dispersive tail is infinite. But it is compatible with the theoretical prediction $\gamma_2 = -1$ and the L_∞ norm of the difference between x_m and its fit is still of order 10^{-2} . A similar procedure for the L_2 norm of u_x leads to $\gamma_3 = -1.0004$ and $C_3 = 13.884$ and also match very well with the theoretical prediction. The two control quantities, the L_2 norm of U_ξ and the value of U_ξ at $\xi = 0$ are preserved to the order 10^{-6} and 10^{-4} respectively.

3.2 Small dispersion limit

In this subsection we study initial data of the form $u_0 = \beta \operatorname{sech}^2 x$ for $\epsilon = 0.1$. For $u_0 = 0.3 \operatorname{sech}^2 x$ the energy is positive, the mass is again smaller than the soliton mass, and the critical time (9) is $t_c \approx 74.1577$. No blow-up is expected in this case. To directly integrate gKdV numerically for these initial data we use $N_t = 10^3$ time steps for $t \leq 2t_c$ and $N = 2^{12}$ Fourier modes for $x \in 40[-\pi, \pi]$. As can be seen in Fig. 9, the solution develops a tail of dispersive oscillations towards $-\infty$, the initial data appear to be simply radiated away.

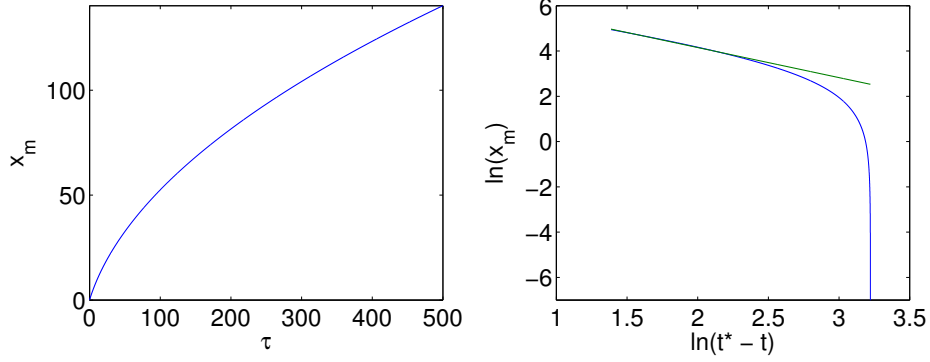


Fig. 8. The position x_m of the maximum of the solution of Fig. 5 as a function of the rescaled time τ on the left and as a function of t and its fit for small values of $\ln(t^* - t)$ on the right.

The L_∞ norm of the solution decreases monotonically. Note that the solution is resolved up to machine precision in Fourier space, and that the numerically computed energy is conserved to the order of 10^{-12} .

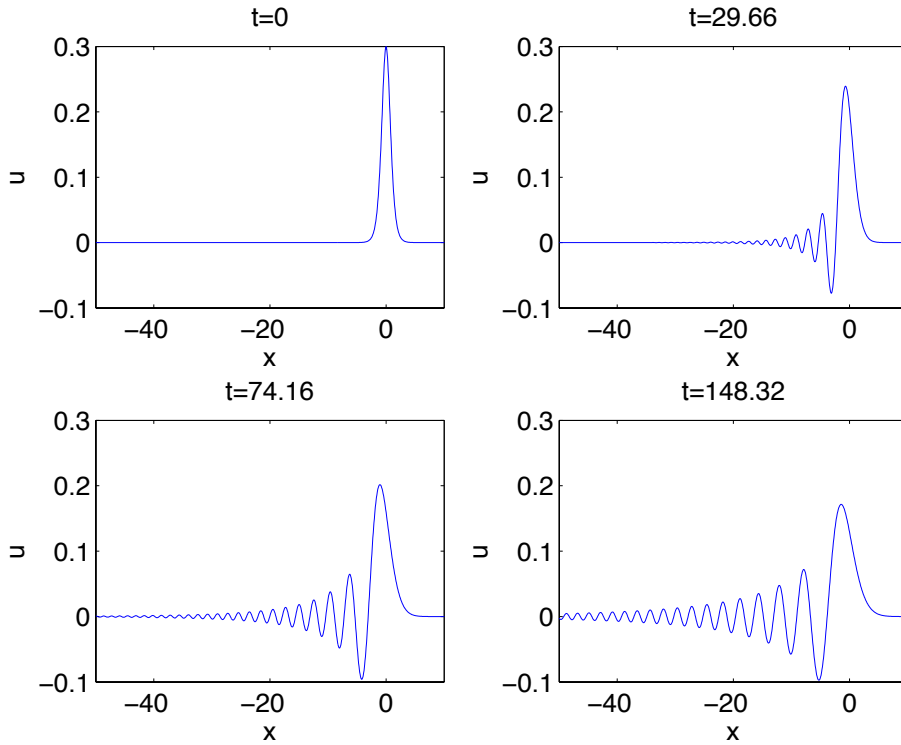


Fig. 9. Solution to the gKdV equation (1) with $\epsilon = 0.1$ for $n = 4$ and the initial data $u_0 = 0.3 \operatorname{sech}^2 x$ for several values of t .

The situation is completely different for $u_0 = \operatorname{sech}^2 x$ for which the energy is negative and for which the mass of the initial data is larger than the soliton mass $M[Q]$. The computation is carried out in this case with $N_t = 2 * 10^5$ time steps for $t < 4.5$ and $N = 2^{14}$ Fourier modes for $x \in 10[-\pi, \pi]$. The

code is stopped at $t = 4.23$ when the energy conservation drops below 10^{-3} and the results are no longer reliable. In contrast to [9], where numerical instabilities stopped the code well before a clear indication of blow-up, we reach with the IRK4 code unambiguously the blow-up regime. The solution is shown for several times in Fig. 10. For small t it is close to the solution of the generalized Hopf equation for the same initial data. The dispersive effects of the third derivative in the gKdV equation become important near the critical time of the generalized Hopf solution. A first oscillation forms at $t \sim t_c$ which then develops into a blow-up as for the perturbed soliton. This is to be compared to the subcritical initial data in Fig. 9. There the dispersive oscillations which also appear in Fig. 10 (where they are hardly visible) are dominant from the beginning. Note that they are numerically fully resolved in both cases in contrast to [7].

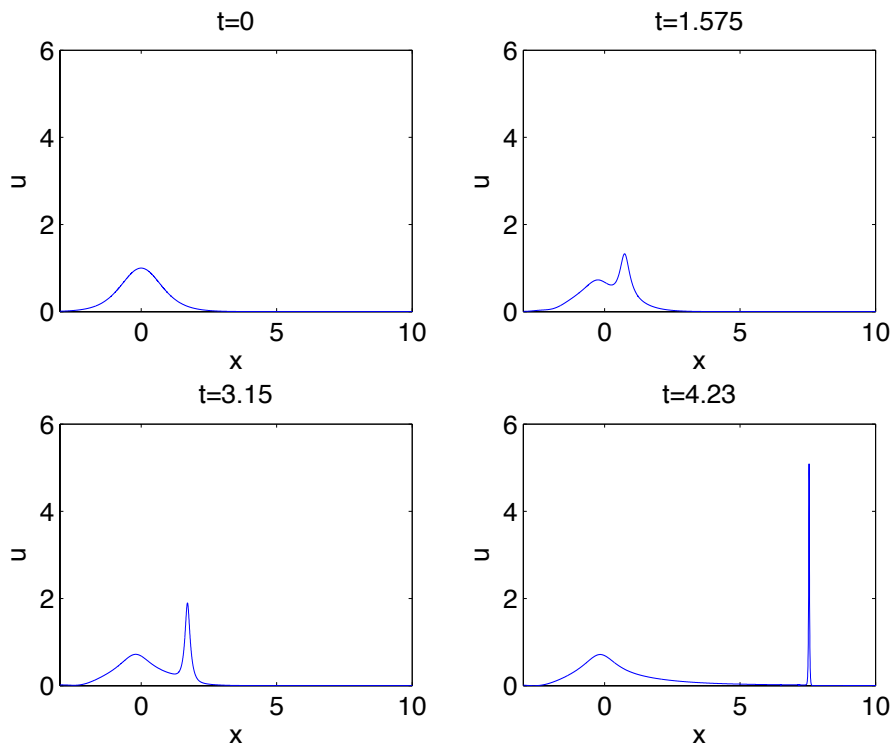


Fig. 10. Solution to the gKdV equation (1) with $\epsilon = 0.1$ for $n = 4$ and the initial data $u_0 = \text{sech}^2 x$ for several values of t . The time of gradient catastrophe for the solution to the generalized Hopf equation is $t_c \approx 0.6007$.

The increase of the L_∞ norm in Fig. 10 can be clearly seen in Fig. 11. As for the perturbed soliton in the previous subsection, the code with the used resolution is not able to get close enough to the blow-up time. Again there is a lack of resolution in Fourier space as can be seen from the Fourier coefficients at the final time in Fig. 11.

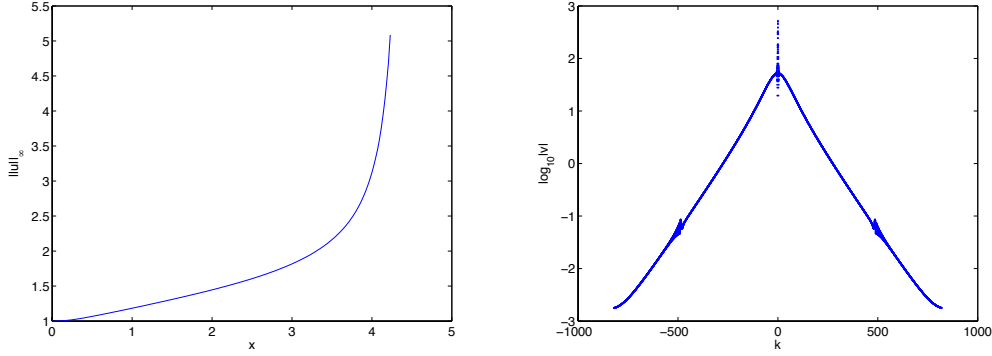


Fig. 11. L_∞ norm of the solution to the gKdV equation (1) with $\epsilon = 0.1$ for $n = 4$ and the initial data $u_0 = \text{sech}^2 x$ in dependence of time on the left, and the modulus of the Fourier coefficients of the solution for $t = 4.23$ on the right.

It does not seem possible to get much closer to the blow-up even with considerably higher resolutions in both time and space. Thus we fit once more the L_∞ norm of the solution close to blow-up to $\ln \|u\|_\infty \sim \alpha \ln(t^* - t) + \kappa$. Doing this for $t > 0.675$ (thus greater than the critical time $t_c \approx 0.6007$ (9) of the generalized Hopf solution), we find $\alpha = -0.4279$, $\kappa = 0.7147$ and $t^* = 4.3554$. The fitting is less good than in the case of the perturbed soliton in the previous subsection (of the order of a few percent) as can be seen in Fig. 12. It indicates a blow-up roughly for $t = 4.35$. The blow-up rate is again compatible with $\|u\|_\infty \sim (t^* - t)^{-1/2}$ as in theorem 1 for perturbations of the soliton, indicating that the blow-up mechanism given there is valid for more general localized initial data than the class \mathcal{A} (4).

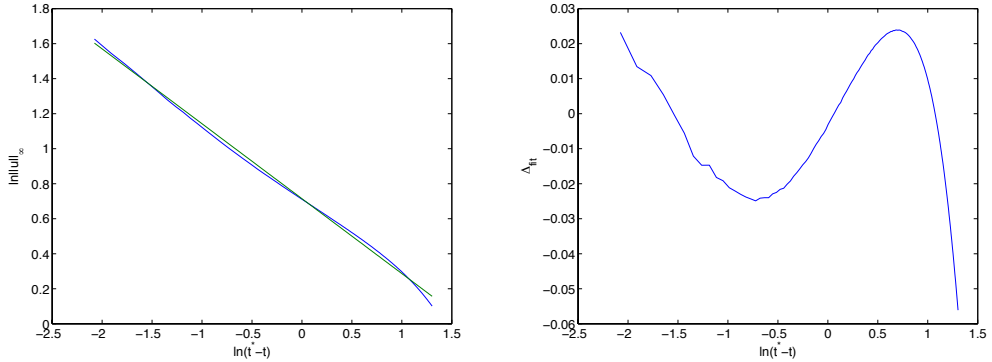


Fig. 12. The logarithm of the L_∞ norm of the solution in Fig. 10 and the fitted curve $\alpha \ln(t_c - t) + \kappa$ on the left, and the difference Δ_{fit} between both curves on the right.

To analyze the blow-up in more detail, we solve again the dynamically rescaled gKdV equation (16). With $N = 2^{14}$ Fourier modes for $\xi \in 120[-\pi, \pi]$ and $N_t = 6 * 10^6$ time steps for $\tau \leq 1700$, we get the solution shown in Fig. 13. It can be seen that the initial data decompose into the rescaled soliton and a remainder which appears to be ultimately radiated away. The Fourier coeffi-

icients in Fig. 13 show the resolution up to machine precision of the solution. The computed relative energy is conserved to the order of 10^{-4} .

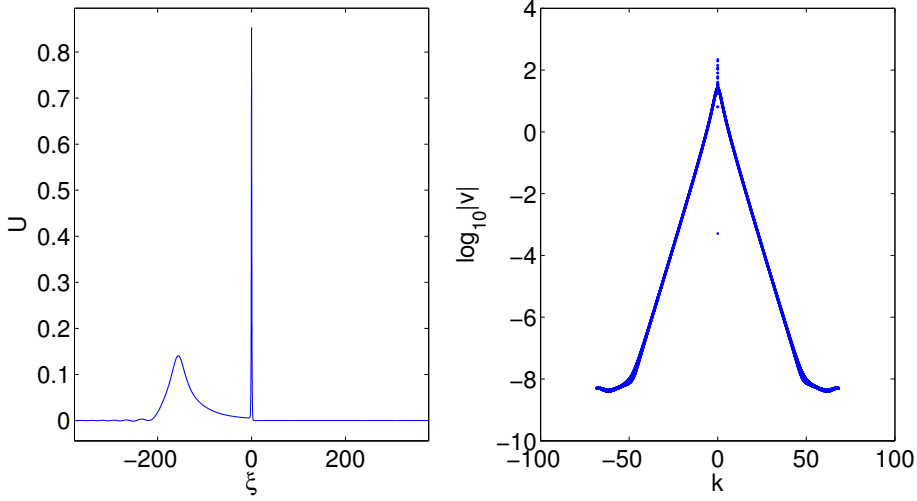


Fig. 13. The solution $U(\xi, \tau)$ of the equation (16) for the initial data $U(\xi, 0) = \text{sech}^2\xi$ for $n = 4$, $\tau = 1700$ (physical time: $t = 4.1787$) and $\epsilon = 0.1$ on the left and the corresponding Fourier coefficients on the right.

The function $a(\tau)$ for the solution in Fig. 13 is shown in Fig. 14. Note that there are no spurious oscillations here in contrast to the perturbed soliton in Fig. 6. This is due to the more rapid decrease of the initial data with x which implies the same behavior for the radiation which caused the oscillations in Fig. 6 due to the imposed periodicity in the computation. We remark that the difference between $a(1700)$ and $a(1530)$ is of the order of 10^{-5} . From $a(\tau)$ we get $L(\tau)$ as shown in Fig. 15 where also a least square fit is given for $L = m\tau + L_0$. We find $m = -0.1673$ and $L_0 = 0.7412$ and thus the blow-up time $t^* = 4.4316$. The difference of the fitted line and L is of the order of 10^{-2} for $t > 2$.

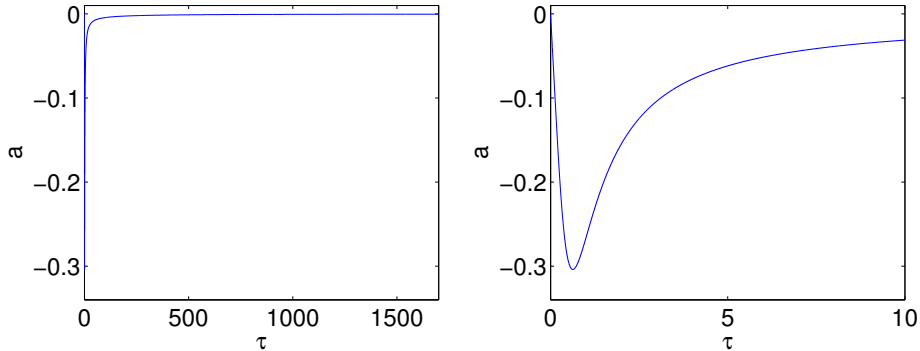


Fig. 14. The function $a(\tau)$ on the whole computed τ -range (left) and a close-up in the interval $\tau \in [0, 10]$ (right) for the solution of Fig. 13.

The physical time t in dependence of τ can be seen in Fig. 15 on the right.

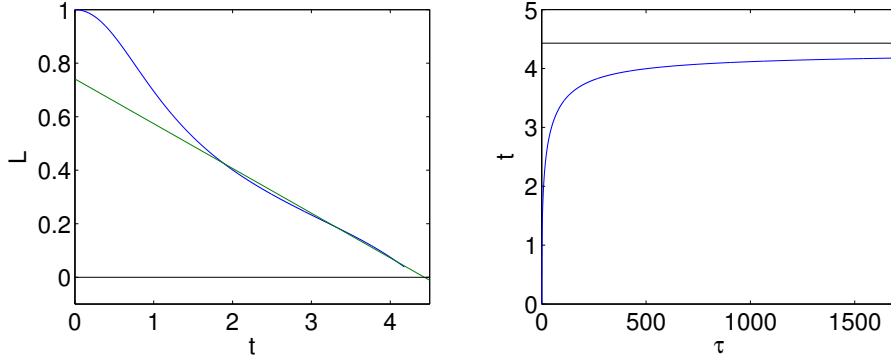


Fig. 15. The scaling factor L as a function of the physical time t and its fit for $t > 2$ (left). The right figure shows the physical time as a function of the rescaled time τ . The black horizontal line in the right figure is the blow up time t^* determined from the fitting of L . Both figures correspond to the solution in Fig. 13.

The position x_m of the maximum of the solution in dependence of t is shown in Fig. 16. For small $t^* - t$ it can be fitted to a straight line $\ln x_m = \gamma_2 \ln(t^* - t) + \ln(C_2)$. We find $\gamma_2 = -0.9117$ and $C_2 = 1.6683$. Thus the maximum shows the same scaling as the L_2 norm of u_x , i.e., the same behavior as for the soliton perturbations in theorem 1. This gives a strong indication that the type of blow-up of this theorem might be generic for much larger classes of localized initial data than treated in the theorem. The results of the fitting for $\|u_x\|_2$ are $\gamma_3 = -1.1921$ and $C_3 = 1.0921$ and therefore also match with the blow-up mechanism of theorem 1 which would imply $\gamma_3 = -1$. The conservation of the numerically computed energy and the L_2 norm of U_ξ is of the same order as for the soliton perturbation.

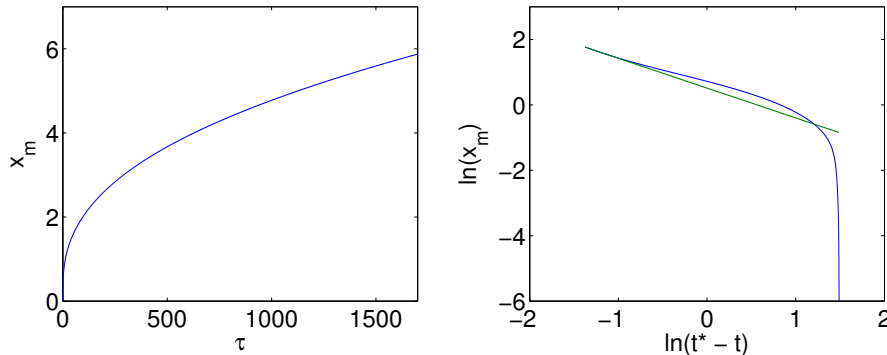


Fig. 16. The position x_m of the maximum for the solution of Fig. 13 as a function of τ on the left and in dependence of t and its fit for small $t^* - t$ to a straight line on the right.

4 The supercritical case $n = 5$

In this section we study as in the previous section perturbations of the soliton and the semiclassical limit for masses in the vicinity of the soliton mass (up to three times this mass). The results can be summarized as follows (see conjecture 3):

- Localized positive smooth initial data with a single maximum and small mass are radiated away.
- Initial data of the same class with sufficiently large mass show self similar blow-up according to (10).

4.1 Perturbations of the soliton

For $n = 5$ and $\epsilon = 1$, the energy of the soliton is $E[Q] = 0.5526\dots$ and the mass is $M[Q] = 4.9738\dots$. Perturbing the soliton as for $n = 4$, i.e., considering initial data of the form $u(x, 0) = \sigma Q(x + 3)$ on a large domain, $x \in 100[-\pi, \pi]$ with $N = 2^{14}$ Fourier modes and $N_t = 10^4$ time steps, we find for $\sigma = 0.99$ again that the soliton is radiated away. The energy of the perturbed initial data is larger than the one of the soliton, the mass smaller. The numerically computed energy is conserved to better than 10^{-12} . It can be seen in Fig. 17 that dispersive oscillations propagating to the left form immediately and eventually appear to radiate the initial data away. The amplitude of these oscillations decreases very slowly which makes the use of a large computational domain necessary. It can be seen that the L_∞ norm of the solution for the perturbed soliton decreases monotonically.

For initial data with $\sigma = 1.01$, the soliton is as in the critical case unstable against blow-up though the energy in the considered example is positive, but smaller than the soliton energy, and the mass is larger than the soliton mass. But this time the blow-up is approached much more rapidly as can be inferred from Fig. 18. We compute for $x \in 100[-\pi, \pi]$ with $N = 2^{14}$ Fourier modes and $N_t = 2 * 10^5$ time steps. The code breaks at $t \approx 1.885$ since the iteration is not converging. The numerically computed energy is still conserved to better than 10^{-8} at $t = 1.88$. Note that the precise blow-up time will be determined below.

It is clear from Fig. 19 that sufficient resolution in Fourier space is no longer given near blow-up. Overall the way the blow-up is approached is different from the case $n = 4$, the loss of resolution in both space and time happens on very small $t^* - t$ scales. The L_∞ norm of the solution for the perturbed soliton is monotonically increasing which also indicates a blow-up, see Fig. 19.

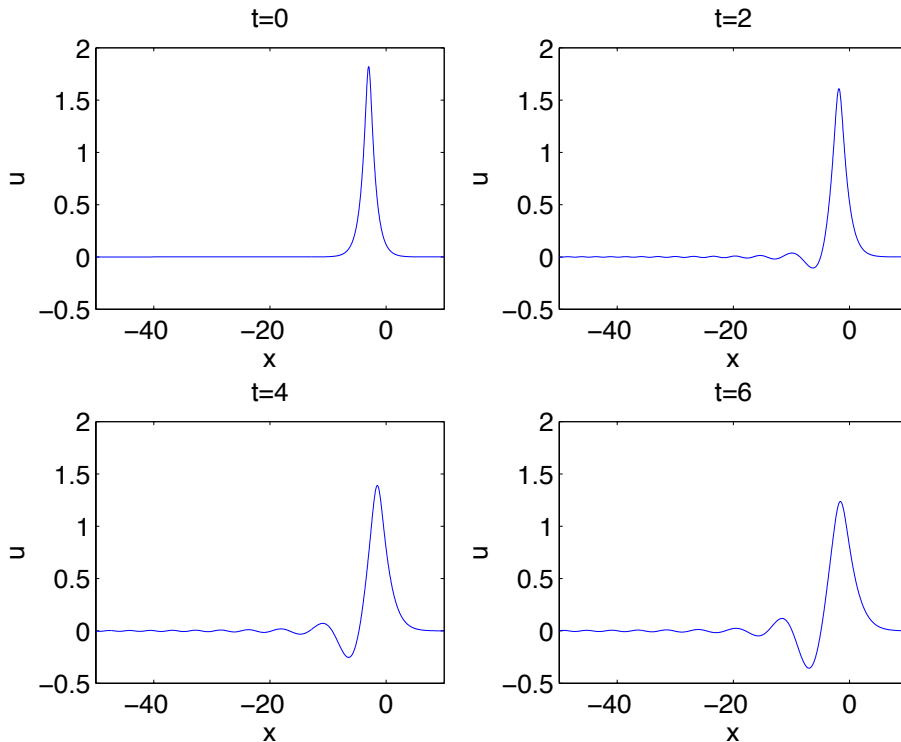


Fig. 17. Solution to the gKdV equation (1) with $\epsilon = 1$ for $n = 5$ and the perturbed soliton initial data $0.99Q(x + 3)$ (3) for several values of t .

Note that the type of blow-up is very different from the one in the L_2 critical case for the perturbed soliton in Fig. 3. There the L_2 norm is invariant under the rescaling (15), and the blow-up profile has essentially the mass of the initial data. In the case $n = 5$ the L_2 norm of the part of the solution blowing up vanishes in the limit $t \rightarrow t^*$ as follows from (21). This can be recognized already in Fig. 18 where the mass escapes to the left of the peak. To study the blow-up in more detail, we again use dynamic rescaling and solve gKdV in the form (16). With $N = 2^{16}$ Fourier modes for $\xi \in 800[-\pi, \pi]$ and $N_t = 2 * 10^6$ time steps for $\tau \leq 12$, we obtain the solution shown in Fig. 20. Since the mass of the solution spreads out to the left of the peak, we shift the initial data to the right to allow longer simulation times (the code typically breaks if the modulus of the solution at the boundaries of the computational domain is of the order of 10^{-3}). We fix the location of the maximum at $\xi_0 = 1884.88$. The Fourier coefficients which can be seen in the same figure indicate that the solution is well resolved. The relative computed mass is conserved to better than 10^{-4} (as before, the relative computed energy is conserved only to the order of 4%). Our results here are in accordance with the ones by Bona et al. [3] as well as Dix and McKinney [7] in what concerns the blow-up. But in contrast to these works, also the dispersive radiation is fully resolved for all recorded values of t .

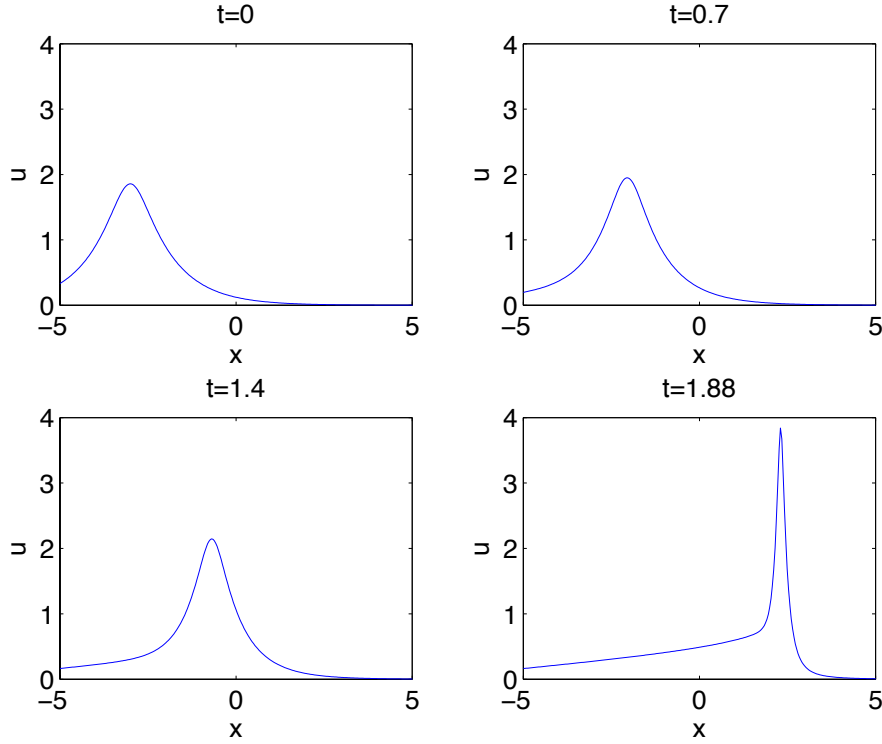


Fig. 18. Solution to the gKdV equation (1) with $\epsilon = 1$ for $n = 5$ and the perturbed soliton initial data $1.01Q(x + 3)$ (3) for several values of t .

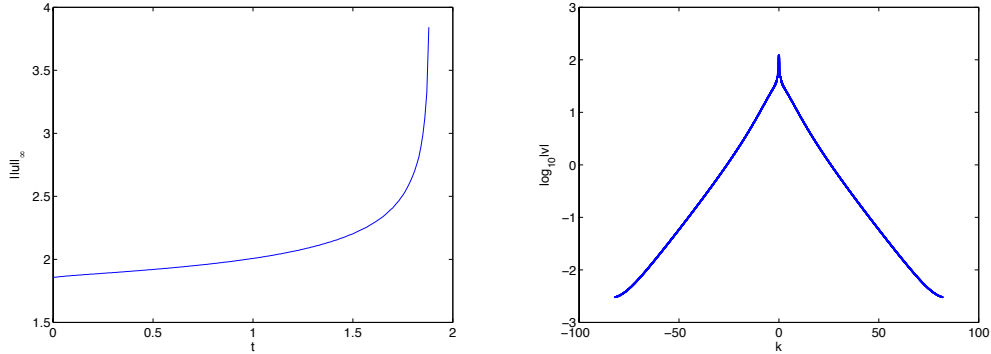


Fig. 19. L_∞ norm of the solution to the gKdV equation (1) with $\epsilon = 1$ for $n = 5$ and the perturbed soliton initial data $1.01Q(x + 3)$ (3) in dependence of time on the left, and the modulus of the Fourier coefficients of the solution for $t = 1.88$ on the right.

The corresponding function $a(\tau)$ can be seen in Fig. 21. As in the case $n = 4$ in Fig. 6, there are small oscillations in a due to the periodic boundary conditions for a which make it hard to read off a precise asymptotic value for $a(\tau)$. But since this value is definitely not zero, the function $L(\tau)$ given in Fig. 23 goes exponentially to zero as can be seen in the logarithmic plot.

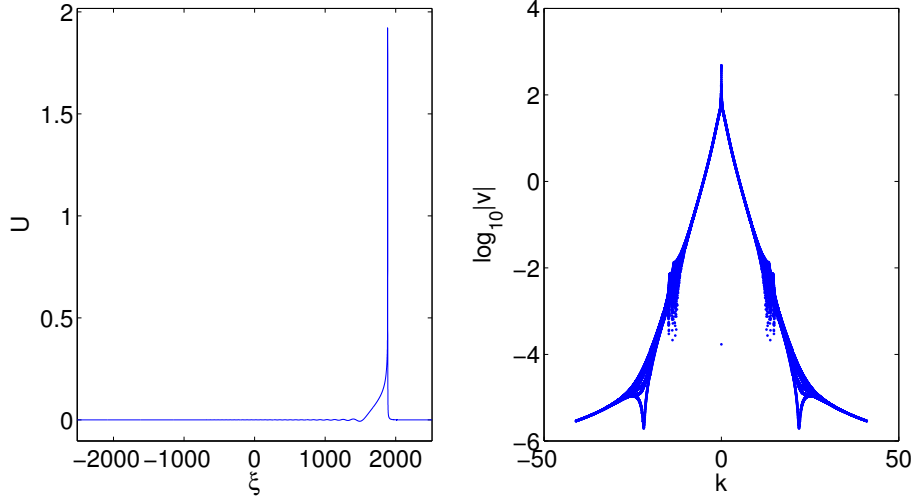


Fig. 20. Solution $U(\xi, \tau)$ of the equation (16) with $n = 5$ for the initial data $U(\xi, 0) = 1.01 Q(\xi)$ (3) for $\tau = 12$ (physical time: $t = 1.8854$) (left) and the corresponding Fourier coefficients (right).

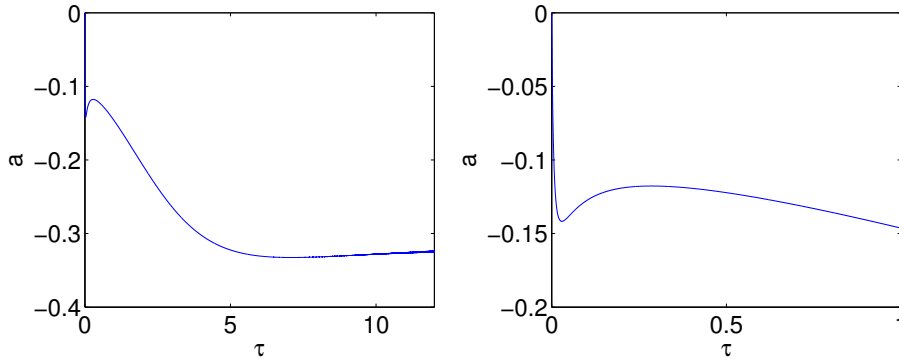


Fig. 21. The function $a(\tau)$ on the whole τ -range (left) and a detailed view of $a(\tau)$ in the interval $\tau \in [0, 1]$ (right) for the solution shown in Fig. 20.

If we consider L as a function of the physical time t , the coordinate transform (15) implies a power law for $L(t)$ (25). In Fig. 22 we can see that in a doubly logarithmic plot $L(t)$ approaches a linear regime. For values $\ln(t^* - t) < -8$ the systems runs into saturation and the corresponding values have to be neglected. We plot the linear part of $\ln L(t)$, $\ln L = \gamma \ln(t^* - t) + C$ and obtain: $\gamma = 0.3281$ and $C = -0.0256$ in accordance with the expectation $\gamma = 1/3$ (25).

In contrast to the case $n = 4$, the blow-up time can directly be read off from the physical time in dependence of τ as can also be seen in Fig. 23. We get the final value $t^* = 1.8854$. The relative change compared to $\tau = 11$ is of the order 10^{-5} . This also shows that the direct integration in this case reaches values of t very close to t^* .

A further difference to the L_2 critical case $n = 4$ is the location of the blow-

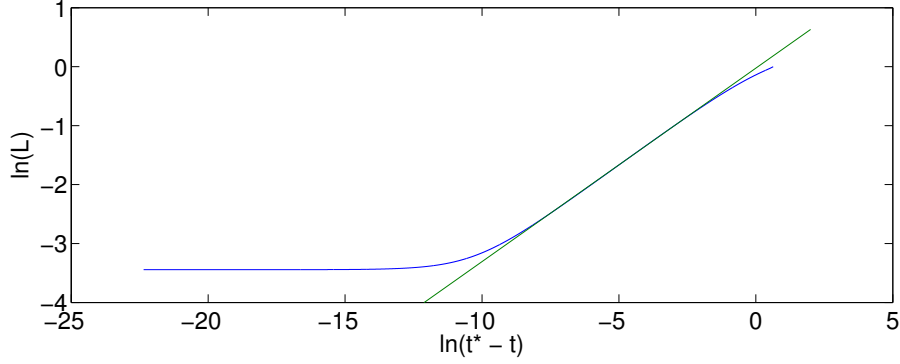


Fig. 22. The scaling factor L in Fig. 20 as a function of the physical time t and its corresponding fit.

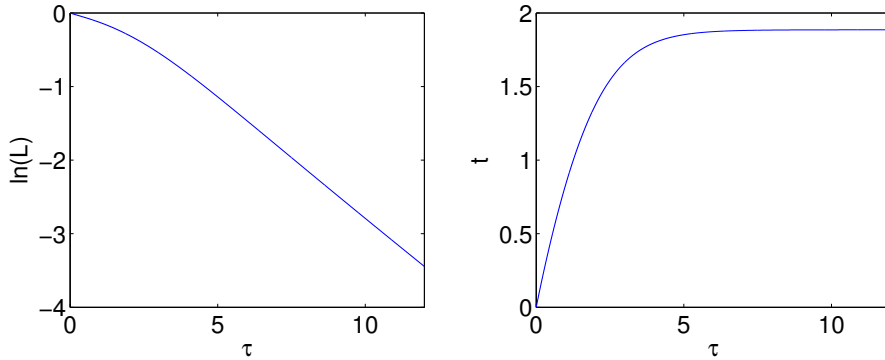


Fig. 23. The scaling factor L (left) and the physical time t (right) as functions of the rescaled time τ for the solution of Fig. 20.

up. Whereas it was infinite in the former case, it is clearly finite for $n = 5$ as can be seen in Fig. 24. Plotting x_m in dependence of the scaling factor L in Fig. 24, one can recognize an essentially linear dependence for small L ($L < 0.4$), i.e., close to blow-up. We get $x_m = \gamma L + x_m^0$ with $\gamma = -5.0665$ and $x_m^0 = 1891.08$, i.e., $\Delta x_m = 6.1983$ which can be interpreted as the blow-up position. The conservation of the numerically computed quantities is here of order 10^{-5} for both the L_2 norm of U_ξ and for the derivative U_ξ at ξ_0 . Since a tends asymptotically to a more negative value than in the other considered examples (for $n = 4$ it tends to zero), comparatively small times τ are sufficient to come close to blow-up. This leads to better numerical results for the computed conserved quantities, but the effect is partially offset by the oscillations in a due to the dispersive radiation and the periodic boundary conditions.

4.2 Small dispersion limit

As for the L_2 critical case $n = 4$ we discuss the initial data $u_0 = \beta \operatorname{sech}^2 x$ in the semiclassical limit $\epsilon \ll 1$. For $\beta = 0.3$ the energy is larger than the soliton

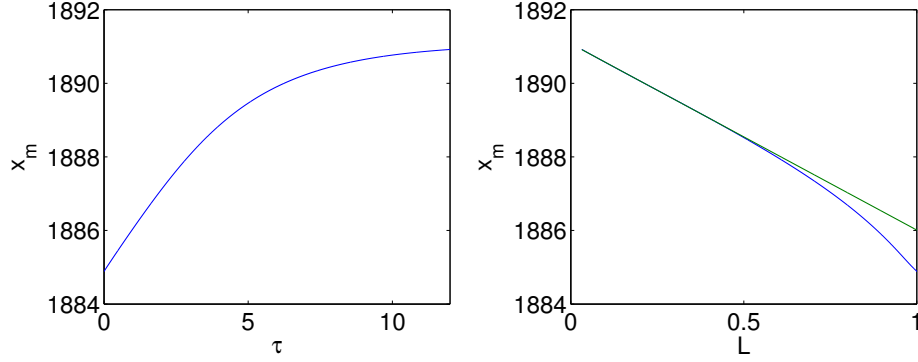


Fig. 24. The position x_m of the maximum of the solution shown in Fig. 20 as a function of the rescaled time τ on the left and in dependence of L on the right, with the corresponding fit.

energy, but positive, the mass is smaller than the mass of the soliton (since the mass has to be rescaled with a factor $1/\epsilon$ to allow comparison with the soliton, it is here equal to 4) and the critical time (9) is $t_c \approx 219.8131$. We use $N_t = 10^4$ time steps for $t \leq 2t_c$ and $N = 2^{12}$ Fourier modes for $x \in 100[-\pi, \pi]$ to directly integrate the gKdV equation for these initial data. As can be seen in Fig. 25, the solution develops again a tail of dispersive oscillations towards $-\infty$. The L_∞ norm of the solution decreases monotonically.

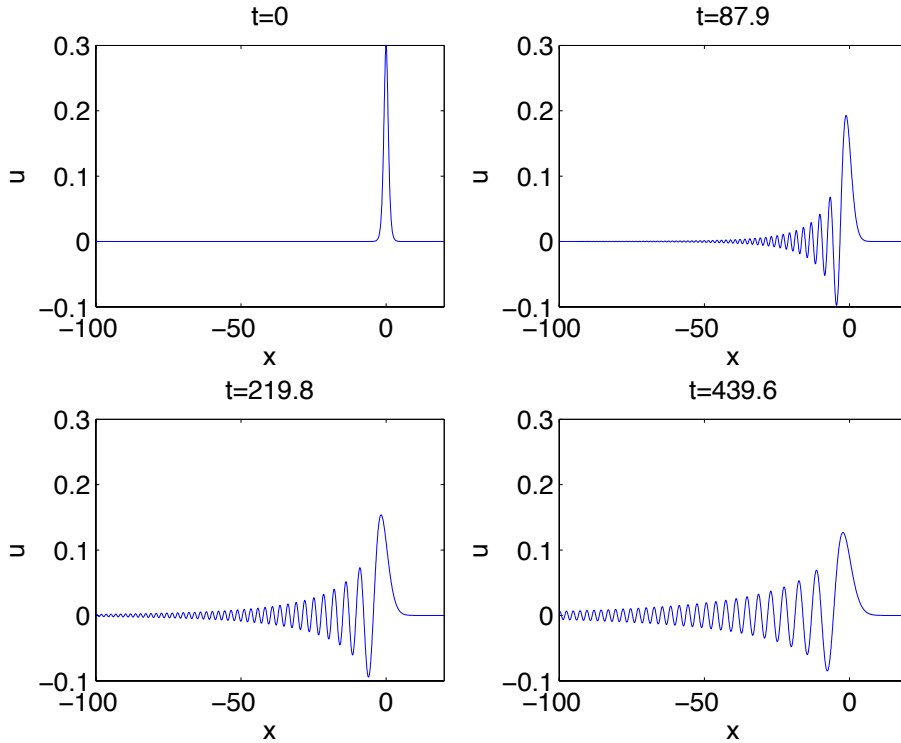


Fig. 25. Solution to the gKdV equation (1) with $\epsilon = 0.1$ for $n = 5$ and the initial data $u_0 = 0.3 \operatorname{sech}^2 x$ for several values of t .

For $\beta = 1$ the energy is again negative, and instead of dispersive radiation dominating as for $\beta = 0.3$, we observe blow-up. The mass of the initial data is again larger than the soliton mass. The computation is carried out in this case with $N_t = 10^5$ time steps for $t < 2.5$ and $N = 2^{14}$ Fourier modes for $x \in 5[-\pi, \pi]$. The code breaks at $t = 2.45$ since the iteration no longer converges. The solution is shown for several times in Fig. 26. For $t \ll t_c \approx 0.5341$ (9) it is very close to the solution of the generalized Hopf equation for the same initial data. The dispersive effects of the third derivative in the gKdV equation become important near the critical time t_c . A first oscillation forms at this time which then develops into a blow-up as for the perturbed soliton. This is to be compared to the subcritical initial data in Fig. 25 where the initial data is just radiated away.

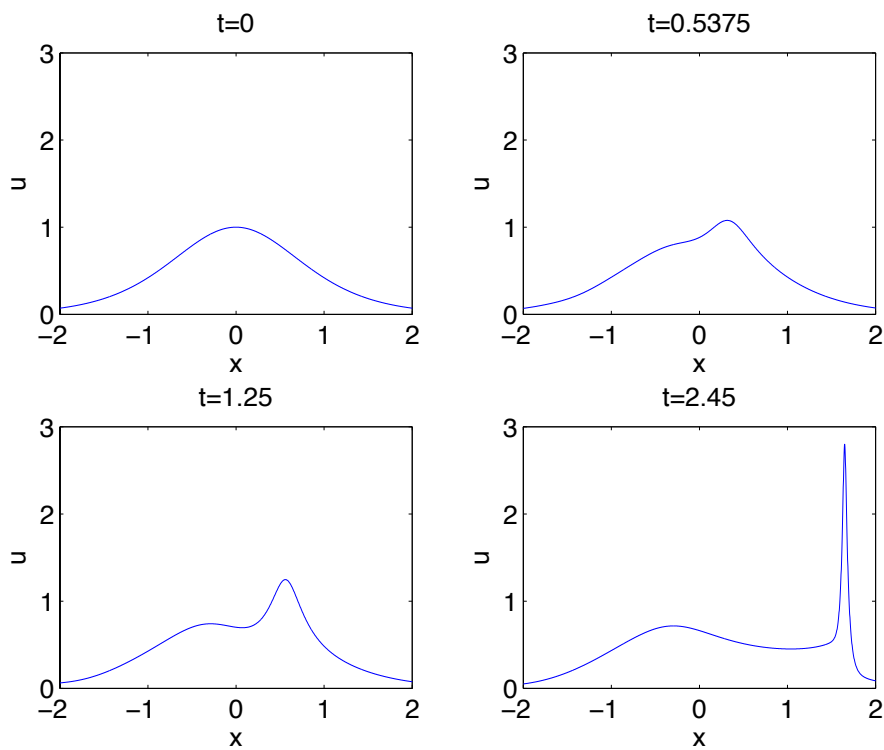


Fig. 26. Solution to the gKdV equation (1) with $\epsilon = 0.1$ for $n = 5$ and the initial data $u_0 = \text{sech}^2 x$ for several values of t .

The monotonous increase of the L_∞ norm in Fig. 26 is even more obvious from Fig. 27. In contrast to the L_2 critical case $n = 4$ we can get very close to the blow-up time. Even for $t \sim t^*$ there is still considerable resolution in Fourier space as can be seen from the Fourier coefficients at the final recorded time in Fig. 27.

To analyze the blow-up in more detail, we study the dynamically rescaled equation (16). We use $N = 2^{14}$ Fourier modes for $\xi \in 130[-\pi, \pi]$ and $N_t =$

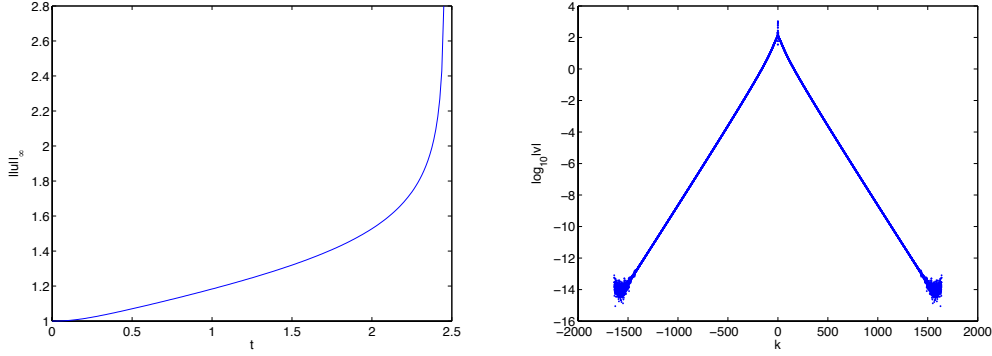


Fig. 27. L_∞ norm of the solution to the gKdV equation (1) with $\epsilon = 0.1$ for $n = 5$ and the initial data $u_0 = \text{sech}^2 x$ in dependence of time on the left, and the modulus of the Fourier coefficients of the solution for $t = 2.45$ on the right.

$6 * 10^6$ time steps for $\tau \leq 200$. The solution at the final time can be seen in Fig. 28 where also the Fourier coefficients are given. They indicate that the solution is well resolved. The relative computed mass containing no derivative is conserved to better than 10^{-4} (as before, the relative computed energy is conserved only to the order of 7%).

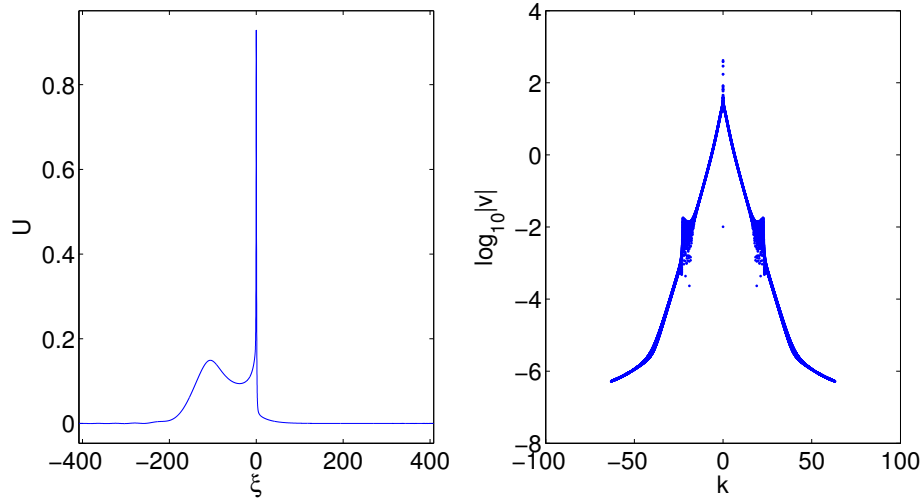


Fig. 28. The solution $U(\xi, \tau)$ for the equation (16) for the initial data $U(\xi, 0) = \text{sech}^2 \xi$ at $\tau = 200$ (physical time: $t = 2.4564$) for $n = 5$ and $\epsilon = 0.1$ (left) and the corresponding Fourier coefficients (right).

The corresponding function $a(\tau)$ tends here clearly to a negative constant as can be seen in Fig. 29. The final value for a is considerably smaller than for the perturbed soliton, $a(200) = -0.0131$, but the relative change compared to $a(180)$ is of the order of 10^{-3} . This indicates that the shown situation is close to blow-up. This can be also seen from the scaling $L(\tau)$ in Fig. 31 which follows for larger τ an exponential law.

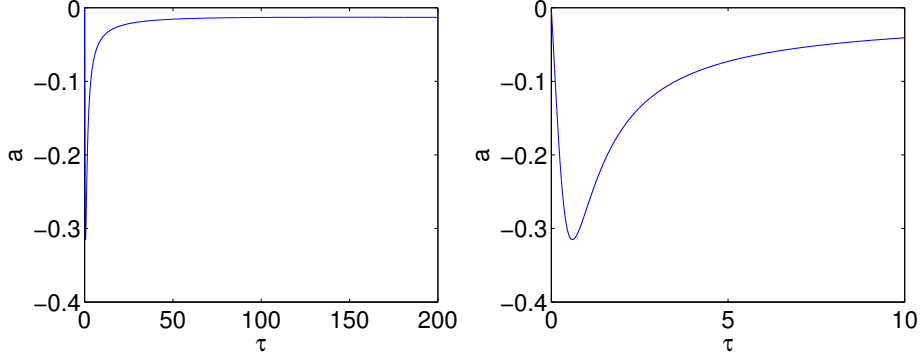


Fig. 29. The function $a(\tau)$ on the whole computed τ -range (left) and a close-up view in the interval $\tau \in [0, 10]$ (right) for the solution of Fig. 28.

As in the case of the soliton perturbation, we also perform a fitting of $L(t)$ to the expected behavior given in formula (25). In Fig. 30 we can see that in a doubly logarithmic plot $L(t)$ approaches the linear regime. For values $\ln(t^* - t) < -8$ the system runs also here into saturation, the corresponding values have to be neglected. We plot the linear part of $\ln L(t)$ and obtain: $\gamma = 0.3316$ and $C = -1.0585$ in accordance with the expectation $\gamma = 1/3$ (25).

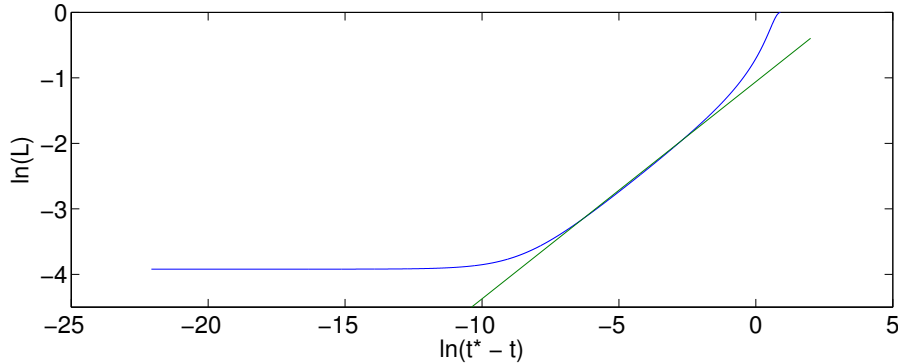


Fig. 30. The scaling factor L in Fig. 28 as a function of the physical time t and its corresponding fit.

The dependence of the physical time on τ can be seen in Fig. 31 on the right. The final value can be again interpreted as the blow-up time $t^* = 2.4564$. The relative change compared to $t(180)$ is of the order of 10^{-5} which confirms that the shown situation is very close to the blow-up.

As before this is not the case for the location x_m of the maximum of the solution as can be seen in Fig. 32, where the asymptotic regime is not yet reached. Plotting x_m as a function of L and fitting it for small L ($L < 0.2$) to a straight line $x_m = \gamma L + x_m^0$, we find $\gamma = -3.3824$ and $x_m^0 = 1.8656$. At the blow-up time t^* , the scaling factor L vanishes, and therefore x_m^0 can be interpreted as the position of the blow-up x^* . The L_2 norm of U_ξ and the value

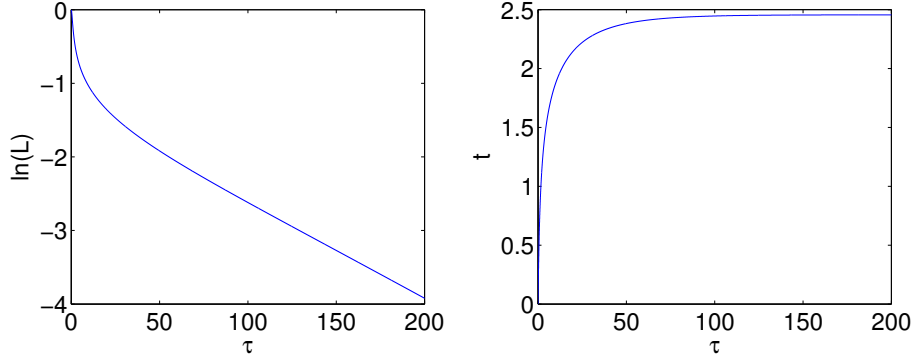


Fig. 31. The scaling factor L (left) and the physical time t (right) as functions of the rescaled time τ for the solution of Fig. 28.

of $U_\xi(0, \tau) = 0$ are both preserved to the order of 10^{-4} .

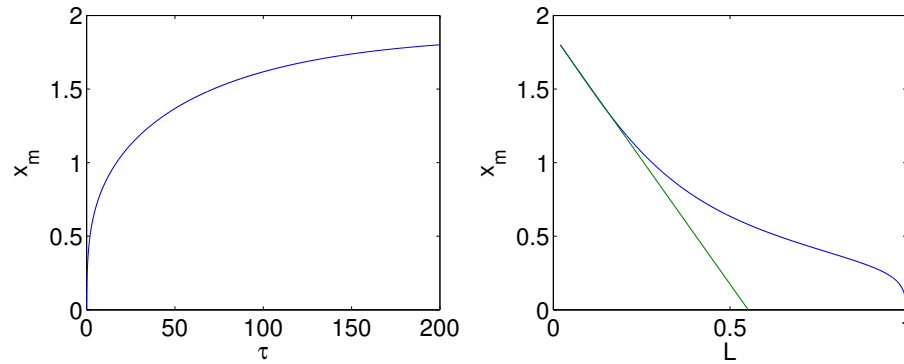


Fig. 32. The position x_m of the maximum of the solution shown in Fig. 28 as a function of the rescaled time τ (left) and in dependence of L (right).

5 Small dispersion limit

In this section we address the case of large masses (more than twice the soliton mass). This allows also to study the small dispersion limit for $\epsilon < 0.1$ for the initial data $u_0 = \text{sech}^2 x$. The results of this study can be summarized as follows (see conjecture 4):

- Localized smooth, positive initial data with a single maximum of large mass show self-similar blow-up as detailed in conjectures 2 and 3.
- The blow-up times for such initial data depend exponentially on ϵ and are strictly greater than the critical time t_c of the corresponding solution to the generalized Hopf equation. This implies there is always a dispersive shock in this case.

Since the dynamically rescaled code is not applicable for large masses for stability reasons as discussed in the previous sections, we directly integrate the gKdV equation and trace the L_∞ norm of u as well as the L_2 norm of u_x . As before the code is stopped once the conservation of the numerically computed energy drops below 10^{-3} indicating that the solution is no longer reliable. For the resulting data, we fit the last 1000 time steps to the expected asymptotic behavior (25) or (26). We consider $\ln \|u_x\|_2^2$ and fit it to $\alpha \ln(t^* - t) + \kappa$. The quantity α is fixed by the theoretical expectation (25) or (26), κ and t^* are determined in a way to minimize $\|\ln \|u_x\|_2^2 - \alpha \ln(t^* - t) + \beta\|_2$. It would be possible to determine also α in this way, but since the result depends very sensitively on t^* especially for the values of t closest to t^* where the numerical accuracy is lowest, this is in practice not a good idea. Instead we check the consistency with an analogous fit for $\|u\|_\infty$. And since we are interested in the ϵ -dependence of t^* , it is mainly important that the estimate for t^* is determined in a consistent way.

5.1 The L_2 critical case $n = 4$

In the L_2 critical case $n = 4$, we solve the gKdV equation for the initial data $u_0 = \text{sech}^2 x$ and $\epsilon = 0.1, 0.09, \dots, 0.001$. We always make first an exploratory run to roughly determine the time, when the code breaks for a given ϵ . Then we run it with $N = 2^{14}$ Fourier modes for $x \in 5[-\pi, \pi]$ and $N_t = 10^5$ time steps to the estimated blow-up time. Only the data with $\Delta < 10^{-3}$ will be considered. For $\epsilon = 0.1$ the solution was shown for different times in Fig. 10. It can be seen that close to the critical time $t_c \sim 0.6007$ (9) one soliton forms which eventually turns into a blow-up. The same situation is considered for $\epsilon = 0.01$ in Fig. 33. It can be seen that in this case several oscillations form before the one appearing first will blow up.

In all cases the codes run out of resolution in Fourier space as can be seen in Fig. 34 where the modulus of the Fourier coefficients is given for the last recorded time with a $\Delta < 10^{-3}$ for $\epsilon = 0.01$. In the same figure we show a close up of the ‘soliton’ (in as light abuse of notation, we call the first oscillation in the following soliton though the latter is not stable and will eventually blow up) blowing up in Fig. 33 at the last recorded time and the rescaled (according to (5) with an appropriate rescaling of x with ϵ) soliton (3). This indicates that the blow-up mechanism of Theorem 1 applies also to initial data with much larger mass than the soliton mass, i.e., to cases not covered by Theorem 1.

The location $x_m(t)$ of the maximum for both solutions can be seen in Fig. 35. It appears that the maximum tends to infinity at blow-up as is rigorously established by [35] for initial data close to the soliton. Thus this seems to be a

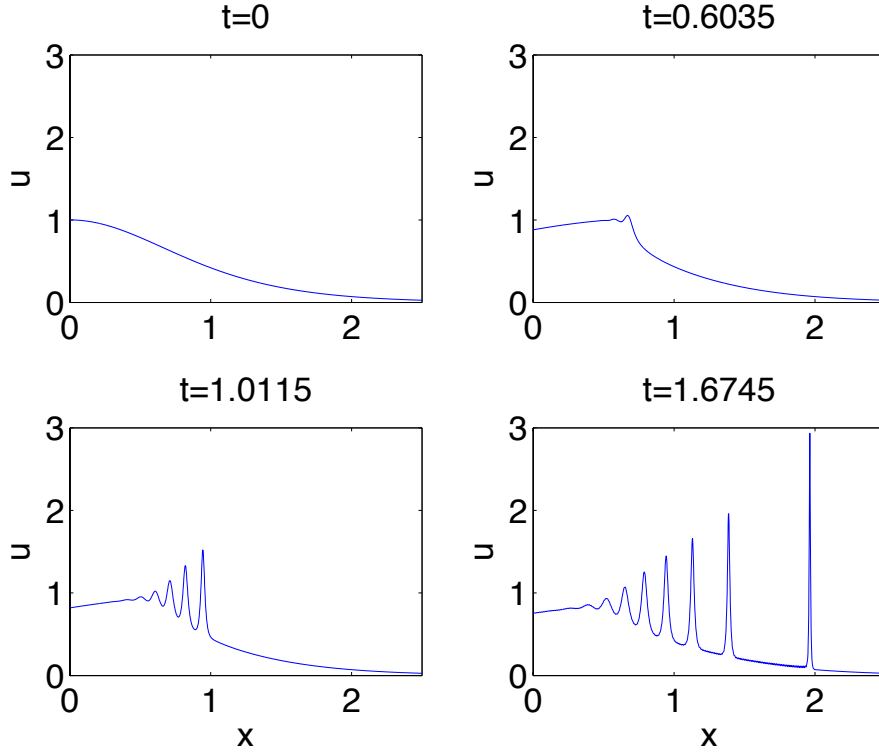


Fig. 33. Solution to the gKdV equation (1) with $n = 4$ for the initial data $u_0 = \text{sech}^2 x$ and $\epsilon = 0.01$ for different times.

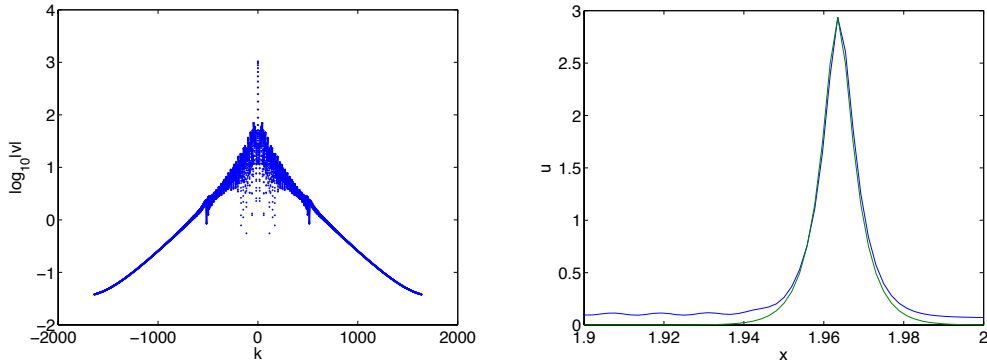


Fig. 34. Modulus of the Fourier coefficients of the solutions to the gKdV equation (1) with $n = 4$ for $\epsilon = 0.01$ for the initial data $u_0 = \text{sech}^2 x$ at the final times shown in Fig. 33 on the left; on the right a close up to the soliton blowing up at $t = 1.6745$ in blue and the rescaled (according to (5)) soliton (3) in green.

rather universal feature for localized initial data with a single maximum. Note, however, that we cannot compute long enough to check this in more detail. It was already seen in section 3 that the predicted asymptotics for x_m is reached considerably later than the one for $\|u_x\|_2$. This is not surprising, since the rescaled soliton will move faster and faster close to blow-up, a behavior that is difficult to catch for any numerical approach.

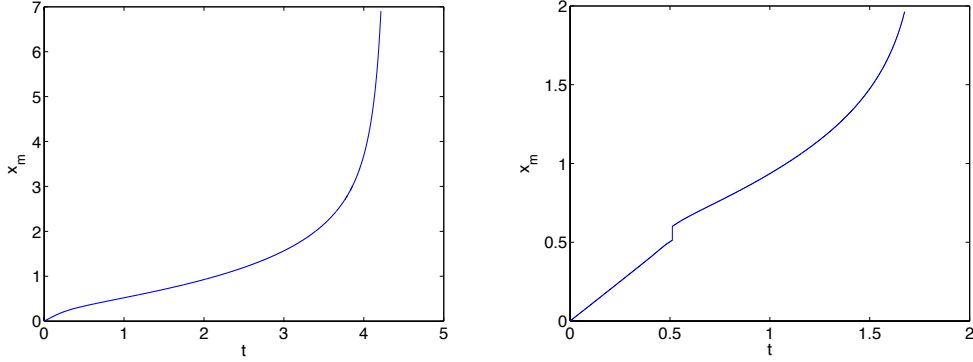


Fig. 35. Location of the maximum of the solutions to the gKdV equation (1) with $n = 4$ for the initial data $u_0 = \text{sech}^2 x$ at the final times shown in Fig. 10 and Fig. 33; on the left for $\epsilon = 0.1$, on the right for $\epsilon = 0.01$.

In Fig. 36 we show the results of the fitting of the logarithm of the various norms to $\alpha \ln(t^* - t) + \beta$. For $\epsilon = 0.1$ we get $t^* = 4.2727$ and $\beta = 10.4555$ for $\|u_x\|_2^2$ and $t^* = 4.2733$ and $\beta = 0.8747$ for $\|u_x\|_\infty$ which shows a remarkable consistency between the two values obtained for t^* . It can be seen that the fitting is worst at early times where the asymptotic regime is not yet reached, and also for $t \sim t^*$ where the accuracy is getting smaller. It can be also recognized that there are small oscillations in the L_∞ norm of u . This is due to the dispersive oscillations propagating to the left and reentering at the right due to the imposed periodicity of the problem, and to the fact that we only determine the maximum on the grid points. This is even more visible for $\epsilon = 0.01$, where the oscillations in the L_2 norm of u_x are considerably smaller than for $\|u\|_\infty$. The fitting gives $t^* = 1.7511$ and $\beta = 11.2375$ in the former case, and $t^* = 1.7398$ and $\beta = 0.3797$ in the latter. Note again the coincidence of the values for t^* despite the strong oscillations in $\|u\|_\infty$.

This procedure is repeated for all values of ϵ we consider. The resulting values of $t^*(\epsilon)$ are then further analyzed. If the conjectured time dependence in [9] proportional to $\epsilon^{4/7}$ close to the critical time t_c were relevant up to blow-up, one would expect an algebraic dependence of t^* on ϵ . But as already mentioned, this cannot really be assumed since the solution of the PI2 equation which is relevant for the asymptotic description close to t_c is regular on the whole real line. In fact we find that a fitting of $\ln(t^*(\epsilon) - t_c)$ to $\gamma \ln \epsilon + \delta$ does not lead to a good correlation. Instead we get as shown in Fig. 37 that there is an exponential dependence of t^* on ϵ . This means that a least square analysis for $\ln(t^*/t_c)$ to $\gamma \epsilon + \delta$ gives $\gamma = 9.7807$ and $\delta = 0.9658$ with standard deviation $\sigma_\gamma = 0.0068$ and a correlation coefficient 0.9995.

This implies not only that $t^* > t_c$, but that $\lim_{\epsilon \rightarrow 0} t^* = t_0^* \sim 1.5780 > t_c \sim 0.6007$. In other words there will be always a gap between the critical time of the generalized Hopf solution and the blow-up time of the corresponding gKdV solution. This is intuitively clear if one looks at the gKdV solutions for different

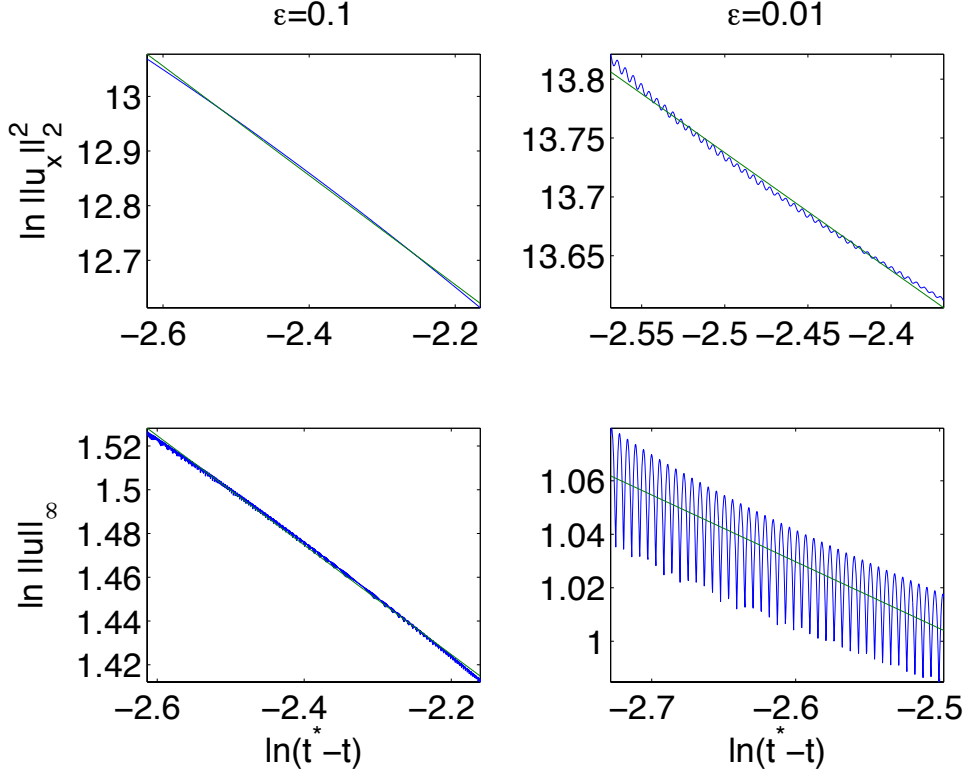


Fig. 36. Fitting of $\ln \|u_x\|_2^2$ and $\ln \|u\|_\infty$ (in blue) to $\alpha \ln(t^* - t) + \beta$ (in green) for the situations shown in Fig. 10 and Fig. 33.

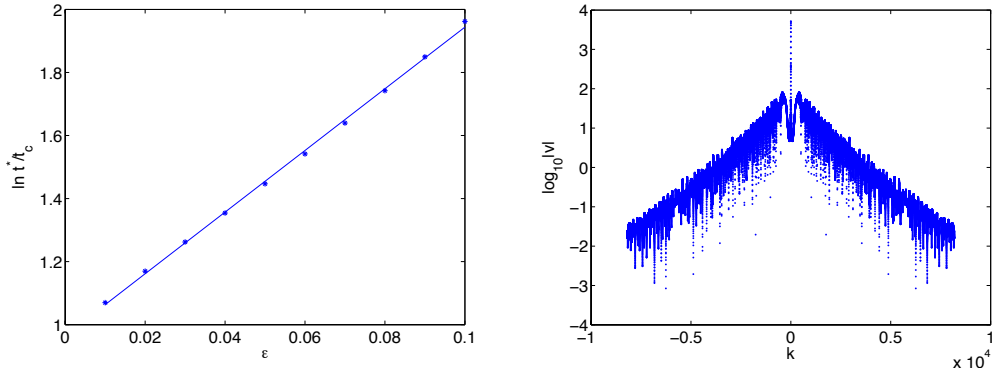


Fig. 37. Least square fit of $\ln(t^*/t_c)$ to $\gamma\epsilon + \delta$ for solutions to the gKdV equation (1) and $n = 4$ on the left; on the right the modulus of the Fourier coefficients for the solution in Fig. 38.

values of ϵ . The smaller ϵ , the more oscillations form before the rightmost soliton blows up. This becomes even more obvious when one looks at even smaller values of ϵ as in Fig. 38. It can be seen that a zone of rapid modulated oscillations as in KdV forms, see for instance [11], for which the rightmost peak eventually blows up. The smaller ϵ , the more oscillations visibly form before this happens, but it appears that the t^* tends to a constant for small ϵ . The calculation is carried out with $N = 2^{16}$ Fourier modes on $x \in 4[-\pi, \pi]$ with

$N_t = 10^5$ time steps. The above fitting procedure for the last 5000 time steps gives for this case a blow-up time $t^* = 1.5427$ which is roughly in accordance with expectations given the numerical inaccuracies (we do not get close enough to blow-up in this case).

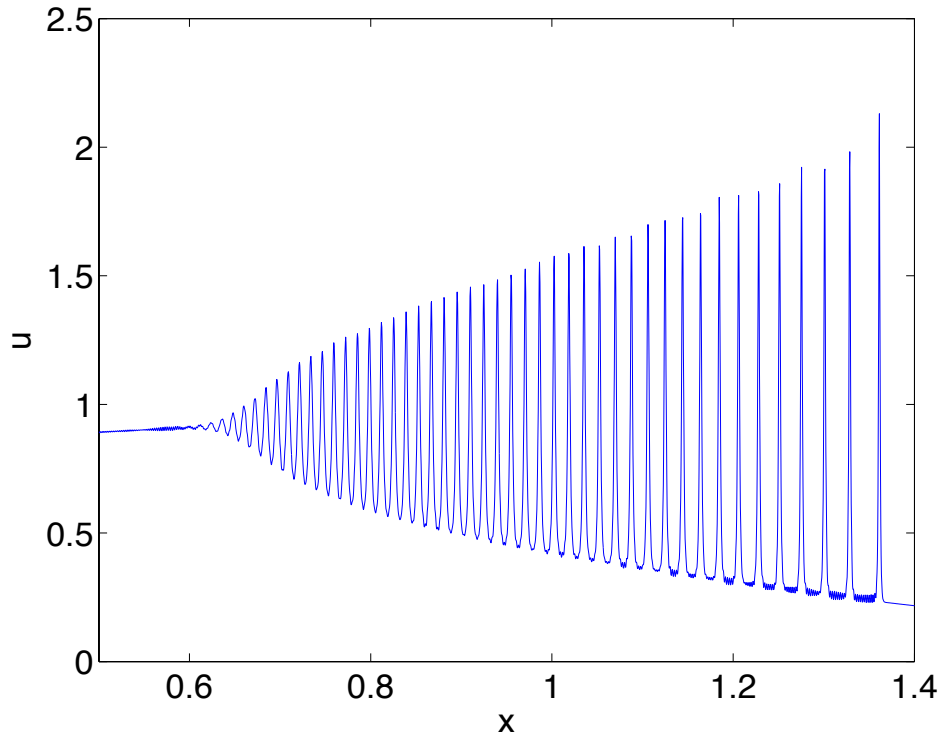


Fig. 38. Solution to the gKdV equation (1) with $n = 4$ for the initial data $u_0 = \text{sech}^2 x$ and $\epsilon = 0.001$ at the final time ($t = 1.33$) for which $\Delta < 10^{-3}$.

The small oscillations which can be seen between the peaks appear to be dispersive oscillations shed from the onset of blow-up. These oscillations are related to the fact that several singularities in the complex plane approach the real axis in this case. As is well known, this leads to oscillations in the Fourier spectrum, see for instance [20] for the small dispersion limit of KdV. The strong oscillations in the Fourier spectrum are clearly visible in Fig. 37 on the right.

5.2 The supercritical case $n = 5$

In this subsection we repeat the considerations for gKdV with $n = 4$ for $n = 5$. The same approaches and parameters are used for the numerical experiments as before. In Fig. 26 the solution for gKdV for the initial data $u_0 = \text{sech}^2 x$ for several values of t was shown. As for $n = 4$ a first oscillation forms close to

the critical time $t_c \sim 0.5341$ (9). This soliton will eventually blow up, and the rest of the hump appears to be radiated away. The same situation is shown for $\epsilon = 0.01$ in Fig. 39. Whereas the type of blow-up is the same as in Fig. 26, several oscillations form before.

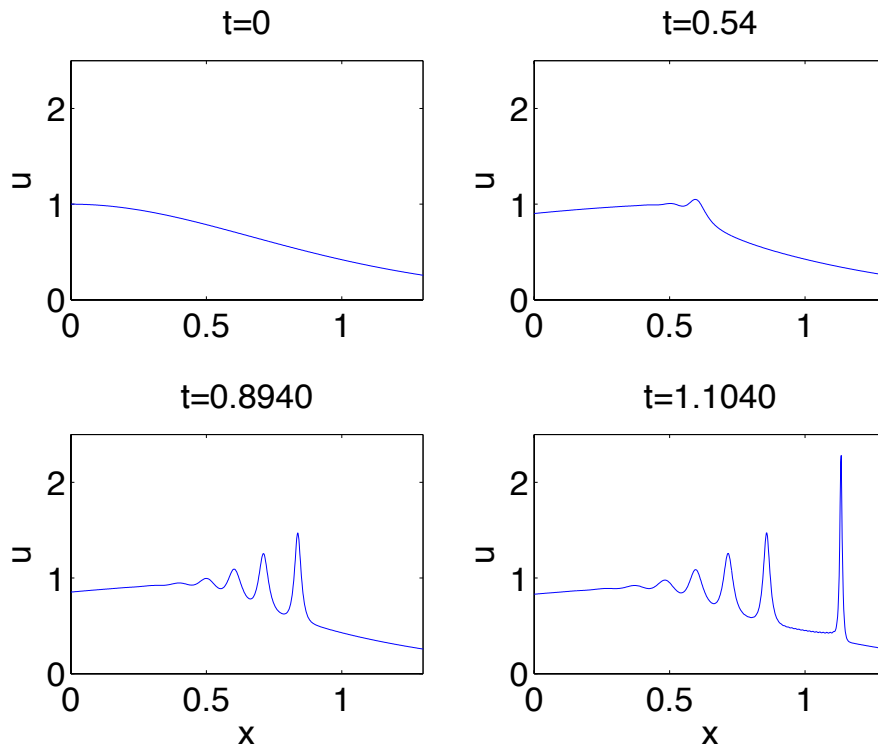


Fig. 39. Solution to the gKdV equation (1) with $n = 5$ for the initial data $u_0 = \text{sech}^2 x$ and $\epsilon = 0.01$ for different times.

Again the codes run out of resolution in Fourier space as can be seen on the left in Fig. 40 where the modulus of the Fourier coefficients is given for $\epsilon = 0.01$ for the last recorded time with a $\Delta < 10^{-3}$. The blow-up is reached here more rapidly than in the case $n = 4$ due to the exponential dependence of the scaling factor L on the rescaled time τ . A close up on the right in Fig. 40 of the rightmost soliton in Fig. 39 illustrates the blow-up profile which is different from the case $n = 4$ in Fig. 34.

The location $x_m(t)$ of the maximum for both solutions can be seen in Fig. 41. Here it is expected from numerical results in [7] (see also section 4) that the blow-up will occur at finite values of x . But again we are not able to compute long enough to obtain conclusive results for x^* .

In Fig. 42 we show the results of the fitting of the logarithm of the various norms to $\alpha \ln(t^* - t) + \beta$. For $\epsilon = 0.1$ we get $t^* = 2.4563$ and $\beta = 1.9253$ for $\|u_x\|_2^2$ and $t^* = 2.4565$ and $\beta = 0.3587$ for $\|u_x\|_\infty$. Again the values for t^* are

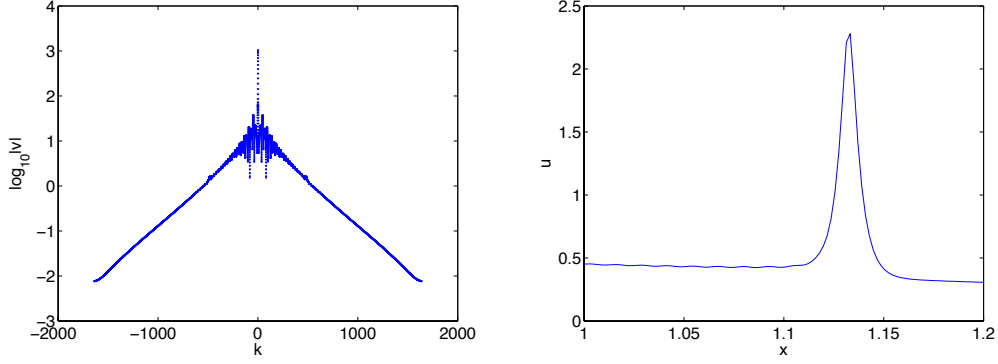


Fig. 40. Modulus of the Fourier coefficients of the solutions to the gKdV equation (1) with $n = 5$ for the initial data $u_0 = \text{sech}^2 x$ for $\epsilon = 0.01$ at the final times shown in Fig. 39 on the left; close up of the soliton blowing up in Fig. 39 on the right.

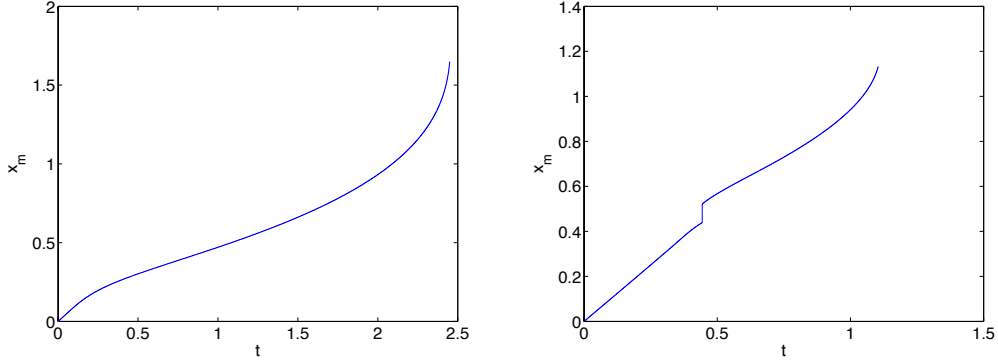


Fig. 41. Location of the maximum of the solutions to the gKdV equation (1) with $n = 5$ for the initial data $u_0 = \text{sech}^2 x$ at the final times shown in Fig. 26 and Fig. 39; on the left for $\epsilon = 0.1$, on the right for $\epsilon = 0.01$.

consistent. Once more the fitting is worst at early times where the asymptotic regime is not yet reached, and also for $t \sim t^*$ where the accuracy is getting smaller. But overall the agreement is much better than for $n = 4$ which is due to the fact that the blow-up is reached in the rescaled time τ exponentially, whereas this happens algebraically for $n = 4$. Also the oscillations in the norms are much smaller than in the latter case. For $\epsilon = 0.01$, the fitting gives $t^* = 1.1475$ and $\beta = 9.2364$ for $\ln \|u_x\|_2^2$, and $t^* = 1.1434$ and $\beta = 0.55821$ for $\ln \|u\|_\infty$. Note again the coincidence of the values for t^* .

The resulting values of $t^*(\epsilon)$ for the remaining values of ϵ are considered in a least square fit. As for $n = 4$ we do not obtain good correlation for an algebraic dependence of t^* on ϵ . But we find also here that a fitting of $\ln(t^*/t_c)$ to $\gamma\epsilon + \delta$ gives $\gamma = 8.4596$ and $\delta = 0.6794$ with standard deviation $\sigma_\gamma = 0.0031$ and a correlation coefficient $r = 0.9999$.

This implies that $\lim_{\epsilon \rightarrow 0} t^* = t_0^* \sim 1.0536 > t_c \sim 0.5341$. Thus there will be also here a gap between the critical time of the generalized Hopf solution and

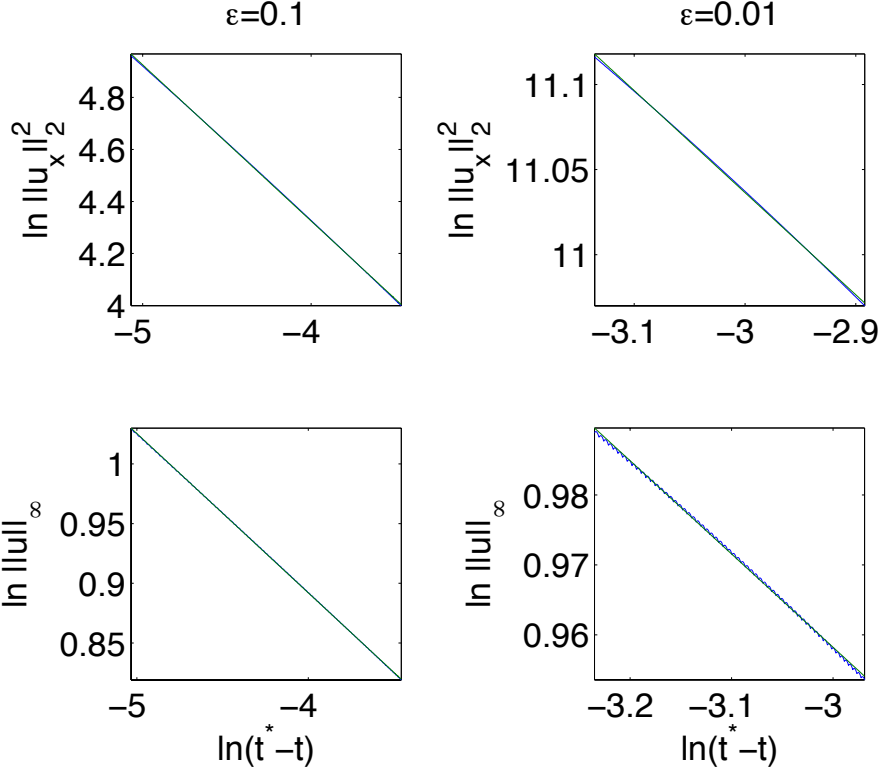


Fig. 42. Fitting of $\ln \|u_x\|_2^2$ and $\ln \|u\|_\infty$ (in blue) to $\alpha \ln(t^* - t) + \beta$ (in green) for the situations shown in Fig. 26 and Fig. 39.

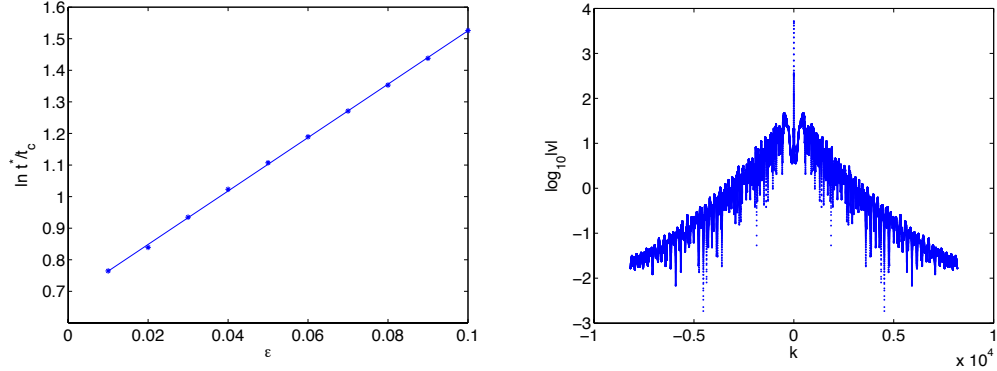


Fig. 43. Least square fit of $\ln(t^*/t_c)$ to $\gamma\epsilon + \delta$ for solutions to the gKdV equation (1) and $n = 5$ on the left; the modulus of the Fourier coefficients for the solution in Fig. 44 on the right.

the blow-up time of the corresponding gKdV solution. In Fig. 44 we show the solution for gKdV with $n = 5$ for the initial data $u_0 = \text{sech}^2 x$ at the final recorded time before blow-up for $\epsilon = 0.001$. Again a zone of rapid modulated oscillations forms before the rightmost oscillation blows up. There are once more small oscillations between the peaks marking the onset of the self similar blow-up. They are related again to oscillations in the Fourier spectrum as can be seen on the right in Fig. 43.

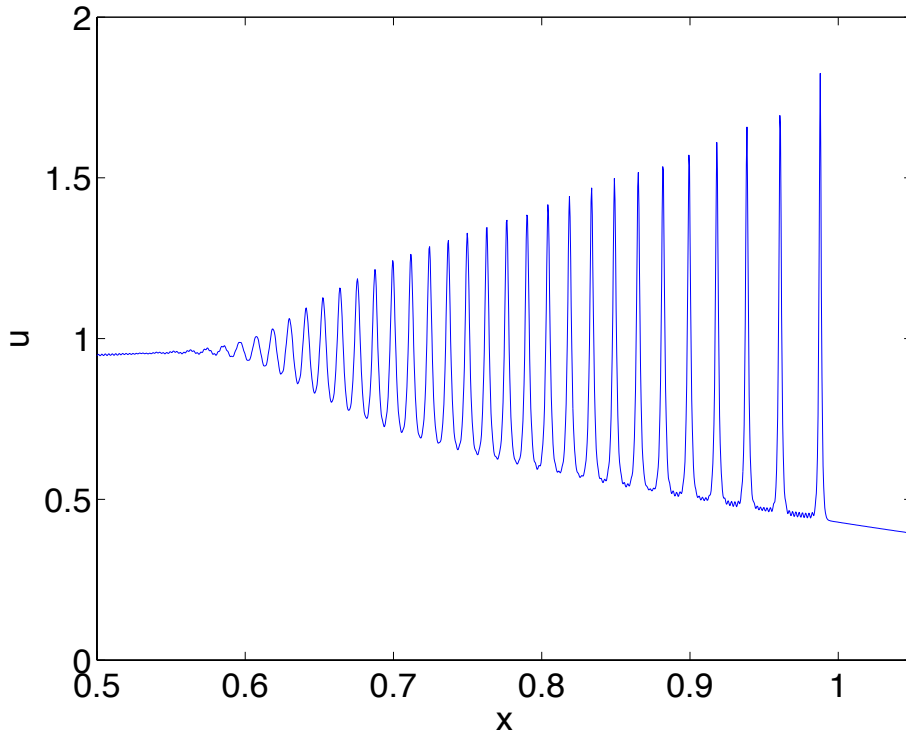


Fig. 44. Solution to the gKdV equation (1) with $n = 5$ for the initial data $u_0 = \text{sech}^2 x$ and $\epsilon = 0.001$ at the final time for which $\Delta < 10^{-3}$.

References

- [1] J. L. Bona, V. A. Dougalis, O. A. Karakashian, Fully discrete Galerkin methods for the Korteweg-de Vries equation, *Comp. & Maths. with Appls.* 12A (7) (1986) 859–884.
- [2] J. L. Bona, V. A. Dougalis, O. A. Karakashian, W. R. McKinney, Computations of blow-up and decay for periodic solutions of the generalized Korteweg-de Vries-Burgers equation, *Appl. Num. Maths.* 10 (3–4) (1992) 335–355.
- [3] J. L. Bona, V. A. Dougalis, O. A. Karakashian, W. R. McKinney, Conservative, high-order numerical schemes for the generalized Korteweg-de Vries equation, *Phil. Trans. R. Soc. Lond. A* 351 (1695) (1995) 107–164.
- [4] J. L. Bona, P. E. Souganidis, W. A. Strauss, Stability and instability of solitary waves of Korteweg-de Vries type, *Proc. R. Soc. Lond. A* 411 (1987) 395–412.
- [5] J. L. Bona, F. B. Weissler, Similarity solutions of the generalized Korteweg-de Vries equation, *Math. Proc. Camb. Phil. Soc.* 127 (2) (1999) 323–351.
- [6] S. M. Cox, P. C. Matthews, Exponential time differencing for stiff systems, *J. Comp. Phys.* 176 (2002) 430–455.

- [7] D. B. Dix, W. R. McKinney, Numerical computations of self-similar blow-up solutions of the generalized Korteweg-de Vries equations, *Differ. Integral Equ.* 11 (5) (1998) 679–723.
- [8] B. Dubrovin, On Hamiltonian perturbations of hyperbolic systems of conservation laws, II: universality of critical behaviour, *Comm. Math. Phys.* 267 (2006) 117–139.
- [9] B. Dubrovin, T. Grava, C. Klein, Numerical study of breakup in generalized Korteweg-de Vries and Kawahara equations, *SIAM J. Appl. Math.* 71 (4) (2011) 983–1008.
- [10] B. Dubrovin, T. Grava, C. Klein, A. Moro, On critical behaviour in systems of Hamiltonian partial differential equations, Preprint available at: [arXiv:1204.4625](https://arxiv.org/abs/1204.4625).
- [11] T. Grava, C. Klein, Numerical solution of the small dispersion limit of Korteweg de Vries and Whitham equations, *Comm. Pure Appl. Math.* 60 (11) (2007) 1623–1664.
- [12] M. Hochbruck, A. Ostermann, Exponential Runge-Kutta methods for semilinear parabolic problems, *SIAM J. Numer. Anal.* 43 (2005) 1069–1090.
- [13] M. Hochbruck, A. Ostermann, Exponential integrators, *Acta Numerica* 19 (2010) 209–286.
- [14] A.-K. Kassam, L. N. Trefethen, Fourth order time-stepping for stiff pdes, *SIAM J. Sci. Comput.* 26 (4) (2005) 1214–1233.
- [15] T. Kato, On the Cauchy problem for the (generalized) Korteweg-de Vries equation, in: I. E. Segal, V. Guillemin (eds.), *Studies in applied mathematics: A volume dedicated to Irving Segal*, vol. 8 of *Advances in Mathematics: Supplementary Studies*, Academic Press, 1983.
- [16] C. E. Kenig, G. Ponce, L. Vega, Well-posedness and scattering results for the generalized Korteweg-de Vries equation via the contraction principle, *Comm. Pure Appl. Math.* 46 (1993) 527–620.
- [17] C. Klein, Fourth order time-stepping for low dispersion Korteweg-de Vries and nonlinear Schrödinger equations, *ETNA* 29 (2008) 116–135.
- [18] C. Klein, R. Peter, Numerical study of blow-up in solutions to generalized Kadomtsev-Petviashvili equations, *Discr. Cont. Dyn. Syst. B* 19(6) (2014) doi:10.3934/dcdsb.2014.19.1689.
- [19] C. Klein, K. Roidot, Fourth order time-stepping for Kadomtsev-Petviashvili and Davey-Stewardson equations, *SIAM J. Sci. Comput.* 33 (6) (2011) 3333–3356.
- [20] C. Klein, K. Roidot, Numerical study of shock formation in the dispersionless Kadomtsev-Petviashvili equation and dispersive regularizations, *Physica D* 265 (2013) 1–25.

- [21] C. Klein, J.-C. Saut, A numerical approach to blow-up issues for dispersive perturbations of Burgers' equation, Preprint available at: [arXiv:1401.1390](https://arxiv.org/abs/1401.1390).
- [22] C. Klein, J.-C. Saut, A numerical approach to blow-up issues for Davey-Stewartson II type systems, Preprint available at: [arXiv:1406.1146](https://arxiv.org/abs/1406.1146).
- [23] C. Klein, C. Sparber, P. Markowich, Numerical study of fractional nonlinear Schrödinger equations, Proc. R. Soc. A 470 (2014) 20140364.
- [24] H. Koch, Self similar solution to super-critical gKdV, Preprint available at: [arXiv:1404.4591](https://arxiv.org/abs/1404.4591).
- [25] N. E. Kosmatov, I. V. Petrov, V. F. Shvets, V. E. Zakharov, Large amplitude simulation of wave collapses in nonlinear Schrödinger equations, preprint from the Space Research Institute Moscow.
- [26] N. E. Kosmatov, V. F. Shvets, V. E. Zakharov, Computer simulation of wave collapses in the nonlinear Schrödinger equation, Physica D 52 (1) (1991) 16–35.
- [27] J. C. Lagarias, J. A. Reeds, M. H. Wright, P. E. Wright, Convergence properties of the Nelder-Mead simplex method in low dimensions, SIAM Journal of Optimization 9 (1998) 112–147.
- [28] M. J. Landman, G. C. Papanicolaou, C. Sulem, P. L. Sulem, Rate of blowup for solutions of the nonlinear Schrödinger equation at critical dimension, Phys. Rev. A 38 (8) (1988) 3837–3843.
- [29] B. LeMesurier, G. Papanicolaou, C. Sulem, P.-L. Sulem, The focusing singularity of the nonlinear Schrödinger equation, in: M. G. Crandall, P. H. Rabinowitz, R. E. L. Turner (eds.), Directions in partial differential equations, vol. 54 of Mathematics Research Center Symposium, Academic Press, 1987.
- [30] Y. Martel, F. Merle, A Liouville theorem for the critical generalized Korteweg-de Vries equation, J. Maths. Pures Appl. 79 (4) (2000) 339–425.
- [31] Y. Martel, F. Merle, Instability of solitons for the critical generalized Korteweg-de Vries equation, Geom. Funct. Anal. 11 (2001) 74–123.
- [32] Y. Martel, F. Merle, Blow up in finite time and dynamics of blow up solutions for the L^2 -critical generalized gKdV equation, J. Amer. Math. Soc. 15 (3) (2002) 617–664.
- [33] Y. Martel, F. Merle, Nonexistence of of blow-up solution with minimal l^2 -mass for the critical gKdV equation, Duke Math J. 115 (2) (2002) 385–408.
- [34] Y. Martel, F. Merle, Stability of blow-up profile and lower bounds for blow-up rate for the critical generalized KdV equation, Ann. Math., Sec. Series 155 (1) (2002) 235–280.
- [35] Y. Martel, F. Merle, P. Raphaël, Blow up for the critical gKdV equation I: Dynamics near the soliton, Preprint available at: [arXiv:1204.4625](https://arxiv.org/abs/1204.4625).
- [36] Y. Martel, F. Merle, P. Raphaël, Blow up for the critical gKdV equation II: Minimal mass dynamics, Preprint available at: [arXiv:1204.4624](https://arxiv.org/abs/1204.4624).

- [37] Y. Martel, F. Merle, P. Raphaël, Blow up for the critical gKdV equation III: Exotic regimes, Preprint available at: [arXiv:1209.2510](https://arxiv.org/abs/1209.2510).
- [38] D. W. McLaughlin, G. C. Papanicolaou, C. Sulem, P. L. Sulem, Focusing singularity of the cubic Schrödinger equation, *Phys. Rev. A* 34 (2) (1986) 1200–1210.
- [39] F. Merle, Existence of blow-up solutions in the energy space for the critical generalized KdV equation, *J. Amer. Math. Soc.* 14 (3) (2001) 555–578.
- [40] G. Papanicolaou, C. Sulem, P. L. Sulem, X. P. Wang, Dynamic rescaling for tracking point singularities: Application to nonlinear Schrödinger equation and related problems, in: R. E. Caflisch, G. C. Papanicolaou (eds.), *Singularities in fluids, plasmas and optics*, vol. 404 of NATO science series C, Kluwer, 1993.
- [41] T. Schmelzer, The fast evaluation of matrix functions for exponential integrators, Ph.D. thesis, Oxford University (2007).
- [42] C. Sulem, P.-L. Sulem, *The nonlinear Schrödinger equation — Self-focusing and wave collapse*, vol. 139 of Applied Mathematical Sciences, 1st ed., Springer, 1999.
- [43] M. I. Weinstein, Nonlinear Schrödinger equations and sharp interpolation estimates, *Comm. Math. Phys.* 87 (1983) 567–576.
- [44] V. E. Zakharov, V. F. Shvets, Nature of wave collapse in the critical case, *JETP Lett.* 47 (4) (1988) 275–278.